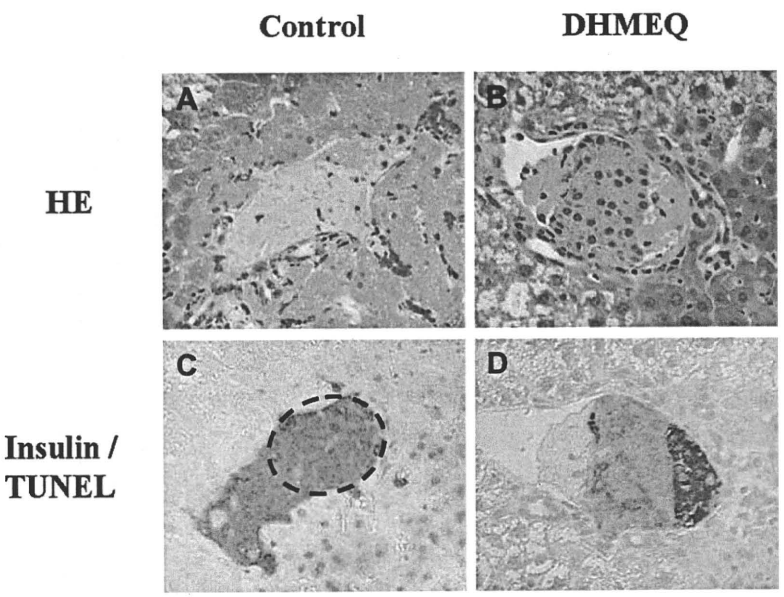

FIG. 9. Histologic analyses of islet-transplanted graft liver. (A), (B) HE, (C), (D) double stainings with insulin and TUNEL of the control and DHMEQ-treated groups were performed. Encircled field indicates TUNEL-positive nuclei within insulin-stained islet cells of the control (C). None of the TUNEL-positive nuclei within insulin-stained islet cells were observed in the DHMEQ-treated group (D). Original magnification, ×200. (Color version of figure is available online.)

accelerates diabetes in NOD mice [30]. Another group has reported that A20 overexpression by NF-κB activation rescues β-cells from FADD-induced cell death [31].

To elucidate the mechanism underlying DHMEQ's prevention of islet apoptosis, we studied the upregulation of cytokines by NF-κB activation because islet-produced MCP-1 was negatively relevant to clinical outcomes such as engraftment and insulin independence [32] and played a role in insulitis by monocyte accumulation [33], or because islet resident macrophages were thought to produce IL-1β in a variety of stimuli that can stimulate NO production by β-cells [34]. Our data indicated that DHMEQ significantly inhibited IL-1β (Fig. 3B) but only slightly inhibited MCP-1; no significant difference was observed between the control and DHMEQ-treated groups. We consider that DHMEQ's inhibitory effect on cytokine expression for the reversal of diabetes would be weak.

We focused on NF-κB's anti-apoptotic effect resulting from its regulation of apoptosis genes. In addition to its important proinflammatory role, NF-κB is a major regulator of cellular apoptosis, but its role was highly controversial [9–11]. Then, the pro-apoptotic gene Bax is considered to be involved in the apoptosis of isolated islets. The ratio of the Bax to the anti-apoptotic gene Bcl-2 might play important roles in the deterioration of insulin secretion and apoptosis after isolation [35–37]. The inhibition of Bax expression might lead to the prevention of apoptosis, the enhancement of islet viability, and the reduction of islet mass to reverse diabetes in mice [36]. So, we investigated Bax and Bcl-2 in isolated islets. Bax was hyperexpressed by the isolation procedure, and DHMEQ inhibited intraislet Bax without inhibiting Bcl-2 expression after isolation (Fig. 4). This means that the isolation procedure tends to induce apoptosis in islets, and that DHMEQ would contribute to the inhibition of islet apoptosis. Another report shows that Bax was regulated by NF-κB through p53 and that the inhibition of NF-κB by a nuclear translocation inhibitor or by genetic manipulation of IκBα or IKK reduced apoptosis and lowered both caspase 3 activity and p53 expression [38]. As is shown in Fig. 6, DHMEQ inhibited caspase3/7 activity compared with the control. Although the relation between NF-κB and p53 in islets is not clear, DHMEQ might inhibit apoptosis by suppressing the caspase pathway through p53 and Bax activity against NF-κB. We considered that the isolation procedure induced islets to activate NF-κB and induced in them a tendency toward apoptosis by the pro-apoptotic gene Bax. DHMEQ would have worked as not only an inhibitor of apoptosis genes, but also as an anti-inflammatory agent to the isolation procedure.

DHMEQ could achieve engraftment by donor pretreatment in marginal islet transplantation (Fig. 7). Previously, we also reported that the inhibition of NF-κB activation in graft liver would promote engraftment by preventing an instant blood-mediated inflammatory reaction (IBMIR) [39]. In this study, islet apoptosis in the controls was nearly 10%, but graft failure was

induced (Fig. 7). This finding suggests that donor pretreatment with DHMEQ might contribute to IBMIR inhibition.

We evaluated islet function *in vivo* by IPGTT, and the AUC of the DHMEQ-treated group was significantly smaller than that of the control group (Fig. 8B). Furthermore, the insulin contents of the DHMEQ-treated group were significantly higher than those of the control (Table 2). Additionally, islets in the DHMEQ-treated grafts were preserved with smaller necrosis, and no apoptosis was found (Fig. 9). This indicates that DHMEQ by donor pretreatment could also contribute to the engraftment of islets in the liver and preserve islet function by inhibiting islet apoptosis.

The cause of apoptosis in islets is not easy to identify, and many NF-κB-dependent genes were considered to be involved in the regulation of apoptosis in islets [40], but their nature remains to be clarified.

In summary, NF-κB in islets was activated immediately after isolation, and DHMEQ, an inhibitor of NF-κB nuclear translocation, inhibited NF-κB activation and prevented apoptosis by down-regulating Bax during isolation, thus improving the engraftment of syngeneically transplanted islets into mouse liver. This indicates that targeting of NF-κB inhibition may be a therapeutic strategy for improving islet transplantation. Other drugs would inhibit NF-κB by inactivation of IκB kinase or phosphorylation of IκB. So, this inhibitory reaction is not specific to NF-κB inhibition, and large doses or gene manipulations are needed to show the inhibitory reaction of NF-κB. However, DHMEQ is specific to nuclear translocation of NF-κB alone by directly attaching the NF-κB subunits, and DHMEQ is not relevant to the phosphorylation of any protein. On the other hand, other drugs, such as antioxidants, aspirin, or pyrrolidine dithiocarbamate, also have reactions to the whole body, and high doses would lead to adverse effects. That is, NF-κB inhibition by these drugs is nonspecific. But, DHMEQ has never been reported to have any adverse effects on small animals. DHMEQ is a small molecular compound and is superior for drug delivery. Thus, we could use it as an apoptosis inhibitor before islet isolation by ductal injection. Further identification of effective treatments for NF-κB inhibition in islet transplantation will be crucial for learning how to prevent β-cell death and how to reduce islet mass to achieve normoglycemia in IDDM.

ACKNOWLEDGMENTS

This study was supported in part by the Program for the Promotion of Fundamental Studies in Health Sciences of the National Institute of Biomedical Innovation (NIBIO) and by a Grant-in-Aid for Scientific Research (no. 18209041) from the Ministry of Education, Culture, Sports, Science, and Technology of Japan. The authors thank Sanae Haga for technical assistance in the NF-κB analysis.

SUPPLEMENTARY DATA

Supplementary data associated with the article can be found in the online version, at doi:10.1016/j.jss.2010.04.044.

REFERENCES

1. Shapiro AM, Lakey JR, Ryan EA, et al. Islet transplantation in seven patients with type I diabetes mellitus using a glucocorticoid-free immunosuppressive regimen. N Engl J Med 2000; 343:230.
2. Ryan EA, Lakey JR, Rajotte RV, et al. Clinical outcomes and insulin secretion after islet transplantation with the Edmonton Protocol. Diabetes 2001;50:710.
3. Paraskevas S, Maysinger D, Wang R, et al. Cell loss in isolated human islets occurs by apoptosis. Pancreas 2000;20:270.
4. Thomas F, Wu J, Contreras JL, et al. A tripartite anoikis-like mechanism causes early isolated islet apoptosis. Surgery 2001; 130:333.
5. Grey ST, Arvelo MB, Hasenkamp W, et al. A20 inhibits cytokine-induced apoptosis and nuclear factor κB-dependent gene activation in islets. J Exp Med 1999;190:1135.
6. Rehman KK, Bertera S, Bottino R, et al. Protection of islets by in situ peptide-mediated transduction of the IκB kinase inhibitor Nemo-binding domain peptide. J Biol Chem 2003;278:9862.
7. Siebenlist U, Franzoso G, Brown K. Structure, regulation and function of NF-κB. Annu Rev Cell Biol 1994;10:405.
8. Johansson U, Olsson A, Gabrielsson S, et al. Inflammatory mediators expressed in human islets of Langerhans: Implications for islet transplantation. Biochem Biophys Res Commun 2003; 308:474.
9. Grimm S, Bauer MK, Baeuerle PA, et al. Bcl-2 down-regulates the activity of transcription factor NF-κB induced upon apoptosis. J Cell Biol 1996;134:13.
10. Osborn L, Kunkel S, Nabel GJ. Tumor necrosis factor α and interleukin 1 stimulate the human immunodeficiency virus enhancer by activation of the nuclear factor κB. Proc Natl Acad Sci USA 1989;86:2336.
11. Beg AA, Baltimore D. An essential role for NF-κB in preventing TNF-α-induced cell death. Science 1996;274:782.
12. Giannoukakis N, Rudert WA, Trucco M, et al. Protection of human islets from the effects of interleukin-1β by adenoviral gene transfer of an IκB repressor. J Biol Chem 2000;275:36509.
13. Baker MS, Chen X, Cao XC, et al. Expression of a dominant negative inhibitor of NF-κB protects MIN6 β-cells from cytokine-induced apoptosis. J Surg Res 2001;97:117.
14. Matsumoto N, Ariga A, To-e S, et al. Synthesis of NF-κB activation inhibitors derived from epoxyquinomicin C. Bioorg Med Chem Lett 2000;10:865.
15. Ariga A, Namekawa J, Matsumoto N, et al. Inhibition of tumor necrosis factor-α-induced nuclear translocation and activation of NF-κB by dehydroxymethylepoxyquinomicin. J Biol Chem 2002;277:24625.
16. Wakamatsu K, Nanki T, Miyasaka N, et al. Effect of a small molecule inhibitor of nuclear factor-κB nuclear translocation in a murine model of arthritis and cultured human synovial cells. Arthritis Res Ther 2005;7:R1348.
17. Suzuki E, Umezawa K. Inhibition of macrophage activation and phagocytosis by a novel NF-κB inhibitor, dehydroxymethylepoxyquinomicin. Biomed Pharmacother 2006;60:578.
18. Wang RN, Rosenberg L. Maintenance of β-cell function and survival following islet isolation requires re-establishment of the islet-matrix relationship. J Endocrinol 1999;163:181.

19. Emamaullee JA, Shapiro AM. Factors influencing the loss of β-cell mass in islet transplantation. Cell Transplant 2007;16:1.
20. Montolio M, Téllez N, Biarnés M, et al. Short-term culture with the caspase inhibitor z-VAD.fmk reduces β cell apoptosis in transplanted islets and improves the metabolic outcome of the graft. Cell Transplant 2005;14:59.
21. Abdelli S, Ansite J, Roduit R, et al. Intracellular stress signaling pathways activated during human islet preparation and following acute cytokine exposure. Diabetes 2004;53:2815.
22. Bottino R, Balamurugan AN, Tse H, et al. Response of human islets to isolation stress and the effect of antioxidant treatment. Diabetes 2004;53:2559.
23. Baeuerle PA, Baltimore D. IκB: A specific inhibitor of the NF-κ B transcription factor. Science 1988;242:540.
24. Kwon G, Corbett JA, Hauser S, et al. Evidence for involvement of the proteasome complex (26S) and NFκB in IL-1β-induced nitric oxide and prostaglandin production by rat islets and RINm5F cells. Diabetes 1998;47:583.
25. Mathews CE, Suarez-Pinzon WL, Baust JJ, et al. Mechanisms underlying resistance of pancreatic islets from ALR/Lt mice to cytokine-induced destruction. J Immunol 2005;175:1248.
26. Kutlu B, Darville MI, Cardozo AK, et al. Molecular regulation of monocyte chemoattractant protein-1 expression in pancreatic β-cells. Diabetes 2003;52:348.
27. Kikuchi E, Horiguchi Y, Nakashima J, et al. Suppression of hormone-refractory prostate cancer by a novel nuclear factor κB inhibitor in nude mice. Cancer Res 2003;63:107.
28. Watanabe M, Ohsugi T, Shoda M, et al. Dual targeting of transformed and untransformed HTLV-1-infected T cells by DHMEQ, a potent and selective inhibitor of NF-κB, as a strategy for chemoprevention and therapy of adult T-cell leukemia. Blood 2005;106:2462.
29. Chang I, Kim S, Kim JY, et al. Nuclear factor κB protects pancreatic β-cells from tumor necrosis factor-α-mediated apoptosis. Diabetes 2003;52:1169.
30. Kim S, Millet I, Kim HS, et al. NF-κB prevents β cell death and autoimmune diabetes in NOD mice. Proc Natl Acad Sci USA 2007;104:1913.
31. Liuwantara D, Elliot M, Smith MW, et al. Nuclear factor-κB regulates β-cell death: A critical role for A20 in β-cell protection. Diabetes 2006;55:2491.
32. Piemonti L, Leone BE, Nano R, et al. Human pancreatic islets produce and secrete MCP-1/CCL2: Relevance in human islet transplantation. Diabetes 2002;51:55.
33. Chen MC, Proost P, Gysemans C, et al. Monocyte chemoattractant protein-1 is expressed in pancreatic islets from prediabetic NOD mice and in interleukin-1β-exposed human and rat islet cells. Diabetologia 2001;44:325.
34. Corbett JA, Wang JL, Sweetland MA, et al. Interleukin 1 β induces the formation of nitric oxide by β-cells purified from rodent islets of Langerhans: Evidence for the β-cell as a source and site of action of nitric oxide. J Clin Invest 1992;90:2384.
35. Mizuno N, Yoshitomi H, Ishida H, et al. Altered bcl-2 and bax expression and intracellular Ca^{2+} signaling in apoptosis of pancreatic cells and the impairment of glucose-induced insulin secretion. Endocrinology 1998;139:1429.
36. Rivas-Carrillo JD, Soto-Gutierrez A, Navarro-Alvarez N, et al. Cell-permeable pentapeptide V5 inhibits apoptosis and enhances insulin secretion, allowing experimental single-donor islet transplantation in mice. Diabetes 2007;56:1259.
37. Thomas D, Yang H, Boffa DJ, et al. Proapoptotic Bax is hyperexpressed in isolated human islets compared with antiapoptotic Bcl-2. Transplantation 2002;74:1489.
38. Kim SJ, Hwang SG, Shin DY, et al. p38 kinase regulates nitric oxide-induced apoptosis of articular chondrocytes by accumulating p53 *via* NFκB-dependent transcription and stabilization by serine 15 phosphorylation. J Biol Chem 2002; 277:33501.
39. Matsumoto S, Matsushita M, Takahashi T, et al. Prevention of intraportal islet graft failure by a Novel NF-κB inhibitor DHMEQ. Transplantation 2006;82(Suppl 3):156.
40. Cardozo AK, Heimberg H, Heremans Y, et al. A comprehensive analysis of cytokine-induced and nuclear factor-κB-dependent genes in primary rat pancreatic β-cells. J Biol Chem 2001; 276:48879.

ELSEVIER

Cancer Genetics and Cytogenetics 201 (2010) 6–14

CANCER GENETICS AND CYTOGENETICS

Array comparative genomic hybridization analysis revealed four genomic prognostic biomarkers for primary gastric cancers

Nobumoto Tomioka[a,*], Keiko Morita[b], Nozomi Kobayashi[a], Mitsuhiro Tada[c], Tomoo Itoh[d], Soichiro Saitoh[b], Masao Kondo[a], Norihiko Takahashi[a], Akihiko Kataoka[a], Kazuaki Nakanishi[a], Masato Takahashi[a], Toshiya Kamiyama[a], Michitaka Ozaki[a,*], Takashi Hirano[b], Satoru Todo[a]

[a]*Department of General Surgery, Hokkaido University Graduate School of Medicine, N-15, W-7, Kita-ku, Sapporo 060-8638, Japan*
[b]*Advanced Industrial Science and Technology-Research Institute for Cell Engineering (AIST-RICE), Tsukuba, Ibaraki, Japan*
[c]*Division of Cancer-Related Genes, Institute for Genetic Medicine, Hokkaido University, Sapporo, Japan*
[d]*Division of Diagnostic Pathology, Kobe University Graduate School of Medicine, Kobe, Japan*

Received 4 October 2009; received in revised form 29 March 2010; accepted 21 April 2010

Abstract Unlike the case with some other solid tumors, whole genome array screening has not revealed prognostic genetic aberrations in primary gastric cancer. Comparative genomic hybridization (CGH) using bacterial artificial chromosome (BAC) arrays for 56 primary gastric cancers resulted in identification of four prognostic loci in this study: 6q21 (harboring *FOXO3A*; previously *FKHRL1*), 9q32 (*UGCG*), 17q21.1~q21.2 (*CASC3*), and 17q21.32 (*HOXB3* through *HOXB9*). If any one of these four loci was deleted, the prognosis of the patient was significantly worse ($P = 0.0019$). This was true even for advanced tumors (stage IIIA, IIB, or IV, $n = 39$) ($P = 0.0113$), whereas only 1 of the 17 patients with less advanced tumors (stage IA, IB, or II; $n = 17$) died of disease after surgery. Multivariate analysis according to the status of four BACs or pathological stage based on the Japanese Classification of Gastric Carcinoma (stages IA, IB, and II vs. stages IIIA, IIIB, and IV) demonstrated that the BAC clone status was also an independent prognostic factor ($P = 0.006$). These findings may help predict which patients with malignant potential need more intensive therapy, or may point to new therapeutic approaches especially for advanced tumors. The parameter here termed the *integrated genomic prognostic biomarker* may therefore be of clinical utility as a prognostic biomarker.

1. Introduction

Gastric cancer is one of the most common malignant solid tumors in the world, and is especially prevalent in East Asia, with >500,000 new patients each year, and >400,000 deaths. In Japan, ~50,000 people die of this disease every year, even now in the 21st century, despite successful early detection, skillful surgery with lymph node dissection, and intensive clinical follow-up with monitoring of serum tumor markers and use of gastrointestinal endoscopy, computed tomography, or positron emission tomography for local and distant metastasis [1,2]. During post-operative observation, we may have to face hepatic or peritoneal metastasis within a couple of years of surgery in some advanced cases. This may be, at least in part, because the present systemic therapeutic approach is unsatisfactory—for example, because of inadequate criteria for deciding eligibility for adjuvant chemotherapy, as well as the questionable efficacy of the chemotherapy itself. We need to know more about the disease to overcome such problems, and to develop therapeutic strategies based on the molecular and biological features responsible for the clinical phenotype of gastric cancer [3–7].

Infection with *Helicobacter pylori* is now accepted as definitely carcinogenic for gastric cancer, and its pathogenic mechanism has been elucidated [8–10]. Nonetheless, cardiac cancer of the stomach is increasing in both western and eastern countries, and it seems to be associated with reflux esophagitis more than with *H. pylori* infection. It can be postulated that gastric cancer arises from inflammatory stimuli to the mucosa, regardless of their cause, which might result in acquisition and accumulation of genomic aberrations in cancer stem cells [11–13]. The hypothesis

* Corresponding authors. Tel.: +81-11-716-1161; fax: +81-11-717-7515.
E-mail addresses: ntomioka@sapporo-shaho.jp (N. Tomioka) or ozaki-m@med.hokudai.ac.jp (M. Ozaki).

0165-4608/$ - see front matter
doi:10.1016/j.cancergencyto.2010.04.017

of cancer stem cell could also apply to gastric cancer [14,15]; however, the predominant cancer cells in clinical lesions seem to have certain aberrations already [16,17]. In fact, we do not know whether the genomic status of the gastric cancer stem cell itself is normal or not.

Even though genetic and epigenetic effects on tumor cells or the cancer stem cell itself still remain to be elucidated, here we analyzed extracted DNA from frozen and dissected primary gastric cancer samples with array comparative genomic hybridization (CGH) [18–20] to identify the genomic aberrations crucial to patient survival status.

2. Materials and methods

2.1. Specimens

Frozen tumor tissue samples of 56 primary gastric cancers were obtained from the Tissue Bank of Hokkaido University Graduate School of Medicine, Department of General Surgery. All surgical specimens in this study were collected in our University hospital from 1999 to 2004 with the consent of the respective patients. Clinicopathological characteristics are given in Table 1. Adjuvant chemotherapy was not given to patients with stage I or II disease, except in one case at the patient's request. Low-dose FP therapy (i.e., 5-fluorouracil–cisplatin) was given to 5 of the 12 patients with stage IIIA or IIIB tumor, resection A or B (i.e., no residual tumor), based on the final findings of curative potential of gastric resection [1], as well as to 7 of the 27 patients with tumor stage IV at their request. Advanced gastric cancers without adjuvant systemic chemotherapy predominate in this patient cohort.

2.2. Extraction of DNA

DNAs were extracted using QIAamp DNA tissue kits (Qiagen, Valencia, CA) from tumor blocks sliced at 200 μm and dissected under magnification. Every fifth slide was stained with hematoxylin and eosin, so that a pathologist could confirm the presence of tumor cells in the samples.

2.3. Array CGH and data processing

The array CGH target slide consists of 4,015 BAC clones printed in duplicate (MacArray Karyo 4K; Macrogen, Seoul, South Korea) on aminosilane-coated slide (CMT-GAPS2 coated slides; Corning, Corning, NY). The Macrogen BAC library is an original library based on the genome of Koreans established in 2000 by Seo of Seoul National University. The average length of insertion is ~100 kb.

Test and sex-matched reference DNAs (500 ng each) were labeled by the random primer method (Bioprime DNA labeling kit; Invitrogen, Carlsbad, CA) for ~16 hours. The probe solution was heated to 70°C for 10 minutes to denature the DNA, then incubated for 60 minutes at 37°C

Table 1
Clinicopathological features of all 56 primary gastric cancers

Tumor stage	Patients, no.	Sex		Depth of tumor invasion[a]					Histological typing[b]					Lymph invasion		Venous invasion		Lymph node metastasis		Resection[c]			Adj Tx		Outcome		
		F	M	m	sm	mp	ss	se	si	pap	tub	por	sig	muc	–	+	–	+	–	+	A	B	C	–	+	Alive	DOD	D_{other}
IA	10	4	6	10	0	0	0	0	0	1	4	2	3	0	10	0	10	0	10	0	10	0	0	10	0	7	1	2
IB	3	1	2	0	1	2	0	0	0	0	1	2	0	0	2	1	2	1	2	1	3	0	0	3	0	2	0	1
II	4	2	2	0	0	1	3	0	0	0	1	3	0	0	1	3	0	4	0	4	3	1	0	3	1	4	0	0
IIIA	8	3	5	0	0	0	3	4	1	0	2	6	0	0	0	8	1	7	1	7	1	6	1	5	3	5	3	0
IIIB	4	2	2	0	0	0	0	4	0	0	2	2	0	0	0	4	0	4	0	4	2	2	0	2	2	1	3	0
IV	27	7	20	0	0	0	4	18	5	2	7	15	1	2	1	26	4	23	4	23	0	5	22	20	7	6	20	1
Total	56	19	37	10	1	3	10	26	6	3	17	30	4	2	14	42	17	39	17	39	19	14	23	43	13	25	27	4

Abbreviations: Adj Tx, adjuvant systemic chemotherapy; DOD, dead of disease; D_{other}, dead of other causes; F, female; M, male.

[a] m, mucosa or muscularis mucosae; sm, submucosa; mp, muscularis propria; ss, subserosa; se, serosa; si, invasion of adjacent structures.

[b] pap, papillary adenocarcinoma; tub, tubular adenocarcinoma (moderately to well differentiated); por, poorly differentiated adenocarcinoma; sig, signet-ring cell carcinoma; muc, mucinous adenocarcinoma.

[c] Resection A, no residual disease with high probability of cure; resection B, no residual disease but not fulfilling criteria for "resection A"; resection C, definite residual disease.

to block repetitive sequences. The array slides were pretreated with salmon sperm DNA in hybridization solution for 30 minutes at room temperature and were mounted on the slide processor (GeneMachines HybStation; Genomic Solutions, Ann Arbor, MI). Hybridization was performed for 40–72 hours on the slide processor with continuous agitation. After a washing, images were acquired with a GenePix 4000A system (Axon Instruments, Sunnyvale, CA), and data analysis was performed using MacViewer (Macrogen) [21,22]. Further statistical analyses were performed with the assistance of biostatistics collaborators (M.T.) at our institution.

The power of sensitivity and ability to distinguish readouts of the MacArray Karyo 4K array is so great that the threshold for the detection of aberration gain or loss is ± 0.1 ($\log_2$ ratio). The basic process is also documented at the Macrogen website (http://www.macrogen.com/eng/biochip/karyochip_process.jsp).

2.4. Real-time quantitative polymerase chain reaction

DNA was extracted from frozen dissected primary samples using a GenElute mammalian genomic DNA miniprep kit (Sigma–Aldrich, St. Louis, MO). The presence of a deletion of interest was detected by real-time quantitative polymerase chain reaction (qPCR) using a QuantiTect SYBR Green PCR kit (Qiagen, Valencia, CA) and LightCycler system for real-time PCR (Roche Applied Science, Indianapolis, IN). For the *AIM1* (6q21), *RGS3* (9q32), *CASC3* (17q21.1), and *ITGB3* (17q21.32) genes, gene-specific primers were designed (Table 2). Each PCR reaction contained 10 μL of PCR mix, 100 ng DNA, 1 μL of each primer, and distilled deionized water to a final volume of 20 μL. Thermal cycling conditions included a preliminary run of 15 minutes at 95°C. Cycle conditions were 40 cycles of 94°C for 15 seconds, 60°C for 20 seconds, and 72°C for 30 seconds.

3. Results

3.1. Genomic biomarkers for prognosis of primary gastric cancers

First, 91 BAC clones with significant copy number aberrations ($P < 0.05$) were selected from 4,015 clones through Cox proportional hazard analysis for 31 primary samples with confirmed apparent predominant composition of >50% cancer in the dissected area of the samples. Box plot and jitter plot analysis for these 91 BAC clones in patients with favorable ($n = 15$) or unfavorable prognoses ($n = 16$) were performed (data not shown). These two prognostic groups (Fig. 1) were selected by computer analysis to yield the greatest significance of the difference repeatedly for overall survival after surgery (i.e., the smallest P-value by log-rank test: $P = 0.0082 \times 10^{-6}$). Of these, 11 BAC clones were identified as including prognostic loci with significant differences between the groups ($P < 0.005$), and 19 clones with lesser but still significant differences between the groups ($P < 0.05$) (data not shown). Survival rates and curves were also analyzed and evaluated on each of these 30 BAC clones separately by log-rank test, resulting in a final selection of four clones as the most reliable and informative prognostic biomarkers in this study (Fig. 2). These clones were significantly underrepresented in tumors with an unfavorable prognosis.

3.2. Genomic biomarkers and clinicopathological prognostic factors for primary gastric cancers

The candidate genes and sequences identified on or flanking the selected BAC clones are listed in Table 3. The first of the four selected clones (#1415) spans 96.7 kb in 6q21. This region contains *FOXO3A* (previously *FKHRL1*) flanked on either side by *PRDM1* [23], *AIM1* [24], *NR2E1* [25], and *CDC40*. The second clone (#2004) spans 96.4 kb in 9q32 and harbors *UGCG* [26], *SUSD1* [27],l and *ROD1*, flanked on either side by *TXN*, *TXNDC8*, and *CDC26* [28], *POLE3* [29], and *RGS3* [30]. The third clone (#3184) spans 102.0 kb in 17q21.1~q21.2 and harbors *CASC3* [31], flanked by *CDC6* [32], *RARA* [33], *GJC1* [34], *TOP2A* [35], and *IGFBP4* [36] on the telomeric side of this clone. The fourth clone (#3215) spans 93.9 kb in 17q21.32 and harbors *HOXB3*, *HOXB4*, *HOXB5*, *HOXB6*, and *HOXB7* [37–40], and *HOXB8* and *HOXB9*, flanked on either side by *CDC27* [41], *ITGB3* [42], *TBKBP1* [43], *TBX21* [44], *PNPO* [45], *CBX1* [46], *SKAP1* [47], and *UBE2Z* [48] and *B4GALNT2* [49].

The status for each of these four clones, along with well-known clinicopathological factors such as tumor thickness,

Table 2
Primers for quantitative polymerase chain reaction

Gene (location)	Forward primer (5′ to 3′)[a]	Reverse primer (5′ to 3′)	Product size (bp)
AIM1 (6q21)	ttcttttagGGGGCACACAG	GGAGTCGATCCACTTTCCAG	205
RGS3 (9q32)	CCTGCAAGTCGACACATGAC	GGGCCAGGATGATGTAGTTG	243
CASC3 (17q21.1)	TGGGAGTCCTCCACAAAGAG	TTCCACAGGCCTAAAACCAG	202
ITGB3 (17q21.32)	CTGTGTGACTCCGACTGGAC	TTAAAGGTGCAGGCATCTGG	191
GAPDH	gcctcactccttttgcagAC	TTCTAGACGGCAGGTCAGGT	243
USP21	ACCCCATGTTACGACCTCTG	ACAGACTTGGAACGGGCTAA	205

[a] Uppercase letters represent the sequence in exon, and lowercase letters represent the sequence in intron.

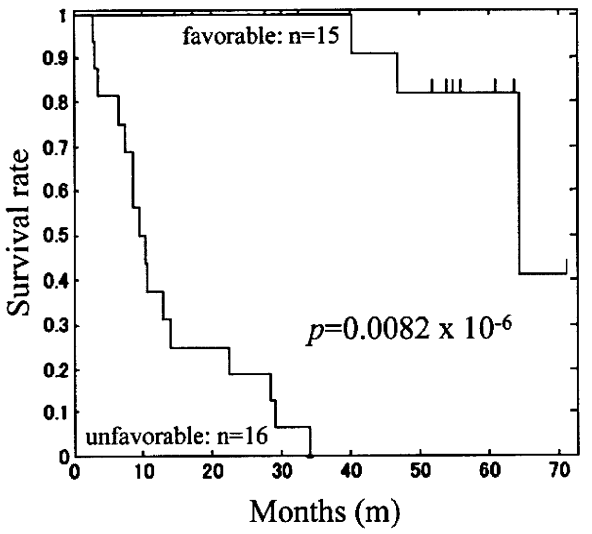

Fig. 1. Survival curves of 31 patients with primary gastric cancers, divided into two groups, favorable and unfavorable, to maximize the significant difference between them in terms of overall survival after surgery (lowest *P*-value by log-rank test = 0.082×10^{-6}).

lymphatic or venous invasion, lymph node metastasis, and terminal staging, all had significant influences on survival, even when univariate analysis was applied (Table 4). If any one of these four clones was lost (i.e., if an integrated genomic prognostic biomarker was positive), prognosis for the patients with tumors having such genomic aberrations remained significantly less favorable in the 31 patients with confirmed predominant cancer composition (P = 0.0004) (Fig. 3A). Furthermore, in the 24 patients with advanced tumors from among these 31 patients (stage IIIA, IIB, or IV, n = 24 vs. stage I or II, n = 7), these biomarkers could distinguish tumors with a further unfavorable prognosis (P = 0.0127) (Fig. 3B). Even for all 56 patients taken together, or the 39 patients with advanced tumors among all the 56 patients, the integrated genomic prognostic biomarker could again distinguish tumors with a less favorable prognosis (P = 0.0019 for the total group and P = 0.0113 for the subset with advanced tumors).

There were no statistically significant differences between patients with favorable vs. unfavorable prognosis on the basis of the BAC biomarkers regarding clinicopathological prognostic and therapeutic factors, with the exception of lymph node metastasis (Table 5). Multivariate analysis for the

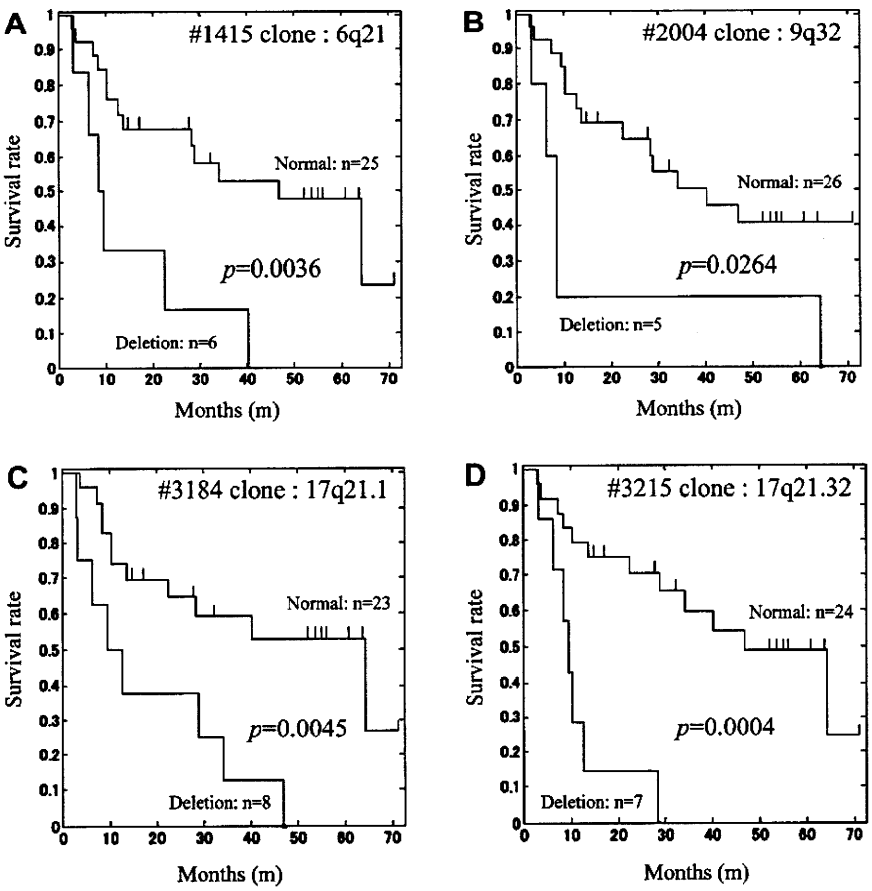

Fig. 2. Survival curves of gastric cancer patients for normal vs. deletion groups at four candidate loci.

Table 3
Summary of candidate genes and sequences located on or flanking the selected BAC clones

BAC ID	Locus	*P*-value	β	BAC start, bp	BAC end, bp	Genes and sequences on or flanking the BAC[a]
#1412	6q21	0.1541562 NS	−1.978217	105717735	105829962	
#1413	6q21	0.0372262	−3.336235	107107668	107200466	*PREP, PRDM1, ATG5* ***AIM1, RTN4IP1, QRSL1*** ***PDSS2, SOBP, SCML4, SEC63, OSTM1***
#1414	6q21	0.0172621	−3.72262	108568947	108658714	***NR2E1, SNX3*** ***LACE1***
#1415[b]	6q21	0.0386686	−2.798985	109087613	109184338	***FOXO3A*** (previously ***FKHRL1***)
#1416	6q21	0.1445321 NS	−2.04327	110694981	110798108	*ARMC2, SESN1, CD164, SMPD2, MICAL1* (previously *NICAL*), *ZBTB24, GPR6, WASF1, CDC40*
#2003	9q32	0.118086264 NS	−3.8148557	111854373	111943831	
#2004[b]	9q32	0.016400085	−6.723210625	112980138	113076490	*TXN, TXNDC8, MUSK, LPAR1* (previously *EDG2*)
#2005	9q32	0.025416175	−4.277062579	114060824	114233134	***OR2K2, KIAA0368, ZNF483, PTGR1*** **(previously *LTB4DH*)**, ***C9orf29, DNAJC25*** **(alias *bA16L21.2.1*)**, ***UGCG, SUSD1, ROD1*** ***ROD1, HSDL2, BC047074*** *C9orf147 (AK131020), KIAA1958, C9orf80, AK128710, AK127013, SLC46A2, CR602666, ZFP37, BC130414, c9orf109 (AL832752), DQ572847, SLC31A2, FKBP15, FKBP15* (previously *KIAA0674*), *SLC31A1, CDC26, PRPF4, RNF183, WDR31, BSPRY, HDHD3, ALAD, POLE3, C9orf43, RGS3*
#2006	9q32	0.082767116 NS	−3.195680005	115352050	115450452	
#3183	17q21.1	0.059700309 NS	−2.581890482	35466118	35565739	
#3184[b]	17q21.1	0.005185929	−5.633345592	35533775	35635800	***CASC3, RAPGEFL1, WIPF2***
#3185	17q21.1	0.012310225	−4.929396269	35573680	35675343	***CDC6***
#3186	17q21.1	0.011229428	−4.199886427	35725837	35829916	***RARA, GJC1, L4737, TOP2A*** *IGFBP4*
#3187	17q21.2	0.392314001 NS	−1.460078597	35871401	35948240	
#3213	17q21.32	0.718287927 NS	−0.467322772	42396082	42464863	*CR602880, CDC27, MYL4, ITGB3, AX748120, C17orf57, BC067758, BC090855, NPEPPS, KPNB1, TBKBP1, TBX21, OSBPL7, MRPL10, LRRC46, SCRN2, SP2, PNPO, PRR15L* (previously *ATAD4*), *CDK5RAP3* (alias *OK/SW-cl.114*), *COPZ2, NFE2L1* (alias *FLJ00380*), *CBX1, SNX11, SKAP1* (previously *SCAP1*)
#3214	17q21.32	0.041832731	−3.065780918	43988355	44111788	***HOXB3, HOXB4, HOXB5, HOXB6, HOXB7, HOXB8, HOXB9***
#3215[b]	17q21.32	0.018379072	−3.456646427	44002394	44096304	***HOXB3, HOXB4, HOXB5, HOXB6, HOXB7, HOXB8, HOXB9,*** *CS444326, PRAC, C17orf93 (AF532777), HOXB13, TTLL6, CALCOCO2, ATP5G1, UBE2Z, SNF8, GIP, IGF2BP1, B4GALNT2, GNGT2, ABI3, PHOSPHO1, NM-001007529, ZNF652*
#3216	17q21.32	0.609317927 NS	−1.018469905	44815976	44940495	

Abbreviations: BAC, bacterial artificial chromosome; NS, not significant.

[a] The reported genes and sequences are those found to be significant. Boldface vs. regular type indicates location on the BAC vs. flanking it.

[b] These four clones (1415, 2004, 3184, and 3215) were determined to be prognostic biomarkers for primary gastric carcinoma.

Table 4
Univariate analysis of clinicopathological and genomic biomarkers on prognosis in 56 primary gastric cancer patients

Prognostic factors	Criteria	*N*	*P*	HR	95% CI
Depth of tumor invasion	≤sm vs. ≤mp	11 vs. 45	0.016	11.671	1.570–86.771
Lymph or venous invasion	− vs. +	11 vs. 45	0.018	11.346	1.528–84.231
Lymph node metastasis	− vs. +	17 vs. 39	0.003	6.119	1.820–20.567
Stage	≤II vs. IIIA≤	17 vs. 39	0.002	24.113	3.259–185.913
Integrated genomic prognostic marker	negative vs. positive	31 vs. 25	0.003	3.338	1.489–7.482
6q21	normal vs. deleted	50 vs. 6	0.001	4.966	1.947–12.667
9q32	normal vs. deleted	49 vs. 7	0.052	2.513	0.992–6.370
17q21.1	normal vs. deleted	42 vs. 14	0.051	2.192	0.995–4.829
17q22.32	normal vs. deleted	45 vs. 11	0.015	2.841	1.223–6.604

Abbreviations: CI, confidence interval; HR, hazard ratio; mp, muscularis propria; sm, submucosa.

integrated genomic prognostic biomarker and pathological stages based on the Japanese classification of gastric carcinoma (stage IA, IB, or II vs. stage IIIA, IIIB, or IV) revealed the former as an independent prognostic factor ($P = 0.006$) (Table 6). Regarding the numbers of deceased patients who had had advanced tumors (stage IIIA, IIIB, or IV), significantly more patients with unfavorable tumors died ($P = 0.0409$), whereas for the patients with less advanced tumors (stage IA, IB, or II), survival after surgery tended to be equally good, even for the patients with tumors positive for the integrated genomic prognostic biomarker ($P > 0.05$, not significant) (Table 7).

3.3. Validation of these four loci by real-time qPCR

In the qPCR analysis, a ratio near 0.5 indicates deletion at the locus. The primers worked for that purpose for 56 primary gastric cancers. The sample GC_35 has no deletion in any of the four loci; by contrast, sample GC_36 has deletion in 6q21, GC_57 in 9q32, GC_54 in both 17q21.1 and 17q21.32 (Fig. 4). The results of real-time qPCR by representative four genes for the loci were compatible with array CGH data.

4. Discussion

Four significant prognostic loci were identified by our statistical analysis of BAC array data of 31 tumors, which segregated all 56 tumors into two groups with significantly more favorable or unfavorable prognosis. These biomarkers enabled us to predict the malignant potential of the tumors and patient course after surgery.

The prognostic locus 6q21 contains *FOXO3*A, which encodes an important regulator of apoptosis and the cell cycle that physically interacts with the transcription factor RUNX3 [50–52]. This is a candidate tumor suppressor frequently lost in gastric cancer cells; it acts on the promoter site for regulating Bim activation essential for the induction of this pathway of apoptosis. *AIM1* [24] encodes the absent in melanoma 1 protein, a novel non-lens member of the βγ-crystallin superfamily, which is associated with tumorigenicity.

The prognostic locus in 9q32 harbors the *UGCG*; this gene encodes UDP-glucose ceramide glucosyltransferase [26] essential for embryonic development and the differentiation of keratinocytes by regulating cell-to-cell or cell-to-matrix interactions, the loss of which might confer

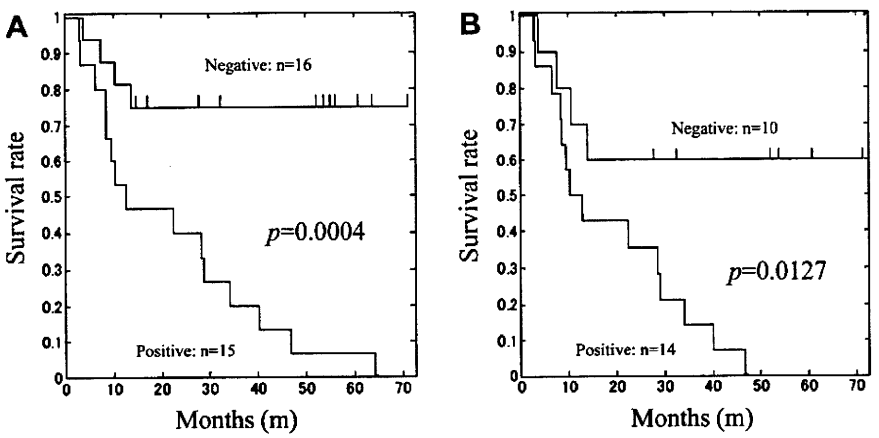

Fig. 3. Survival curves of gastric cancer patients for positive vs. negative integrated genomic prognostic biomarker. (A) All 31 patients with tumors confirmed, apparent predominant composition of >50% cancer. (B) Subset of 24 patients with tumor of stage IIIA, IIIB, and IV from among these 31 patients.

Table 5
Two groups segregated by the integrated genomic prognostic biomarker in 56 primary gastric cancer patients

Genomic prognostic group	Patients, no.	Sex		Depth of tumor invasion[a]					Histological typing[b]					Lymph invasion		Venous invasion		Lymph node metastasis		Stage				Resection[c]		Adj Tx		Outcome		
		F	M	m	sm	mp	ss	se	si	pap	tub	por	sig	muc	–	+	–	+	–	+	IA	IB	II	IIIA	IIIB	IV	A or B	C	IIIA	IIIB	IV	Alive	DOD	D_{other}
Favorable	31	10	21	7	1	3	6	11	3	1	12	14	2	2	11	20	11	20	13	18	7	3	3	6	1	11	21	10	2	1	3	18	9	4
Unfavorable	25	9	16	3	0	0	4	15	3	2	5	16	2	0	3	22	6	19	4	21	3	0	1	2	3	16	12	13	1	1	4	7	18	0
P-value		0.7843		0.328					0.292						0.0634		0.3955		0.0448		0.401						0.1758		0.7881			0.0027		

Abbreviations: Adj Tx, adjuvant systemic chemotherapy; DOD, dead of disease; D_{other} dead of other causes; F, female; M, male.
[a] m, mucosa or muscularis mucosae; sm, submucosa; mp, muscularis propria; ss, subserosa; se, serosa; si, invasion of adjacent structures.
[b] pap, papillary adenocarcinoma; tub, tubular adenocarcinoma (moderately to well differentiated); por, poorly differentiated adenocarcinoma; sig, signet-ring cell carcinoma; muc, mucinous adenocarcinoma.
[c] Resection A, No residual disease with high probability of cure; resection B, No residual disease but not fulfilling criteria for "resection A"; resection C, Definite residual disease.

Table 6
Multivariate analysis of clinicopathological prognostic factors and genomic biomarker in 56 primary gastric cancer patients

Prognostic factors	Criteria	*N*	*P*	HR	95% CI
Stage	≤II vs. ≤IIIA	17 vs. 39	0.002	29.644	3.458–247.689
Integrated genomic prognostic biomarker	negative vs. positive	31 vs. 25	0.006	3.306	1.400–7.804

infiltrating potential. It also contains the *CDC26* gene [28], encoding a subunit of an anaphase-promoting complex that regulates cell division, the loss of which might accelerate proliferation. The *RGS3* gene [30], which is a regulator of G protein signaling 3, might inhibit the silencing of G protein signaling downstream of SDF-1–CXCR4, thereby promoting cell migration.

The locus in 17q21.1 harbors *CASC3* (cancer susceptibility candidate 3) [31], which encodes a component of a conserved protein complex that is essential for mRNA localization in flies and for nonsense-mediated mRNA decay in mammals. *GJC1* [34], located just telomeric to this clone, encodes a gap junction gamma-1 protein, a member of the connexin family essential for gap junction interactions with the second PDZ domain of ZO-1, which is the epithelial tight-junction scaffolding protein associated with CagA, a factor secreted by *H. pylori*. This can result in compromising the integrity of gastric epithelial cells by disrupting junction-mediated functions and could thereby contribute to carcinogenesis.

The locus 17q21.32 harbors the *HOXB3–9* cluster, members of which are associated with many malignant tumors. For example, *HOXB7* [37–40] is expressed at a considerably lower level in several malignancies. *CDC27* [41] encodes a key functional component of the anaphase-promoting complex or cyclosome (APC/C), which could contribute to cell transformation. *ITGB3* (integrin beta 3) [42] regulates apoptosis and adhesion. *SKAP1* (src kinase associated phosphoprotein 1, 55 kDa) [47] enhances integrin-mediated adhesion to both fibronectin and the ICAM-1 protein, so that downregulated *SKAP1* might contribute to tumor cell dispersion. Other possibly relevant genes also flank either side of this clone.

Table 7
Differential distribution of the numbers of deceased primary gastric cancer patients

Genomic prognostic group	Deceased patients, no.	Stage, no. dead of disease/all classified patients					
		Group 1			Group 2		
		IA	IB	II	IIIA	IIIB	IV
Favorable	9	0/7	0/3	0/3	2/6	1/1	6/11
Unfavorable	18	1/3	0/0	0/1	1/2	2/3	14/16
		$P = 0.0631$			$P = 0.0409$		

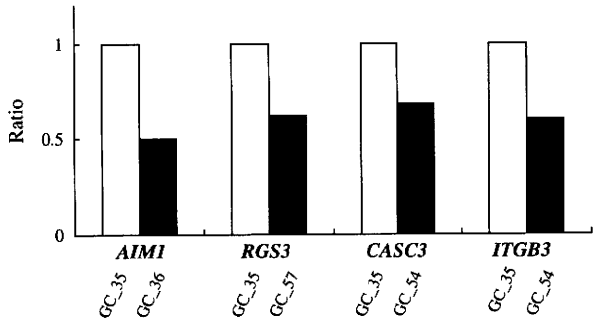

Fig. 4. Quantitative polymerase chain reaction results for representative genes in the four prognostic loci. Gastric cancer sample GC_35 has no deletion, but sample GC_36 has deletion in 6q21 (*AIM1*), GC_57 has deletion in 9q32 (*RGS3*), and GC_54 has deletion in both 17q21.1 (*CASC3*) and 17q21.32 (*ITGB3*).

Depending on whether the remaining wild-type allele is somatically inactivated, lack of the molecules discussed here may or may not contribute to poorer prognosis. Genomic data are not always directly correlated with mRNA expression status, but these nonrandom events seen at the whole-genome level might be associated with phenotype.

In the present study, patients in the unfavorable prognosis group with less advanced tumors could be cured by surgery, but significantly more patients with advanced tumors died. Patients with tumors with loss at any one of the four loci identified here (6q21, 9q32, 17q21.1, and 17q21.32) have a clearly less favorable prognosis. Thus, by applying the prognostic biomarkers identified here, we could predict which advanced tumors had a worse malignant potential. This could be a useful indicator of those patients needing more intensive or new therapeutic approaches.

Further study of the biological implications of these data in terms of the mechanism of acquisition of malignant potential in gastric cancer could lead to improving prognosis or developing better treatments [53].

Acknowledgments

We thank the staff at Advanced Industrial Science and Technology-Research Institute for Cell Engineering (AIST-RICE) for hybridization procedures and for continuous maintenance of the BAC array system. We also thank technical staff at the Tissue Bank, Department of General Surgery, Hokkaido University Graduate School of Medicine, for providing tumor specimens, and staff at the Division of Pathophysiological Science, Hokkaido University Graduate School of Medicine, for the preparation and evaluation of specimens. The authors also acknowledge the New Energy and Industrial Technology Development Organization of Japan (NEDO), which is an incorporated administrative agency for research and development management, the Ministry of Education, Culture, Sports, Science and Technology of Japan, and the Ministry of Health, Labor and Welfare of Japan for the Advancement of Biochemistry for funding this work.

References

[1] Japanese Gastric Cancer Association. Japanese classification of gastric carcinoma: 2nd English edition. Gastric Cancer 1998;1: 10–24.

[2] Japanese Gastric Cancer Association. Therapeutic guidelines for gastric carcinoma. 2nd English ed. Tokyo: Kanehara, 2004: 1–39.

[3] Nørsett KG, Laegreid A, Midelfart H, Yadetie F, Erlandsen SE, Falkmer S, et al. Gene expression based classification of gastric carcinoma. Cancer Lett 2004;210:227–37.

[4] Jinawath N, Furukawa Y, Hasegawa S, Li M, Tsunoda T, Satoh S, et al. Comparison of gene-expression profiles between diffuse- and intestinal-type gastric cancers using a genome-wide cDNA microarray. Oncogene 2004;23:6830–44.

[5] Motoori M, Takemasa I, Yano M, Saito S, Miyata H, Takiguchi S, et al. Prediction of recurrence in advanced gastric cancer patients after curative resection by gene expression profiling. Int J Cancer 2005;114:963–8.

[6] Teramoto K, Tada M, Tamoto E, Abe M, Kawakami A, Komuro K, et al. Prediction of lymphatic invasion/lymph node metastasis, recurrence, and survival in patients with gastric cancer by cDNA array-based expression profiling. J Surg Res 2005;124:225–36.

[7] Tay ST, Leong SH, Yu K, Aggarwal A, Tan SY, Lee CH, et al. A combined comparative genomic hybridization and expression microarray analysis of gastric cancer reveals novel molecular subtypes. Cancer Res 2003;63:3309–16.

[8] Hatakeyama M. Oncogenic mechanisms of the *Helicobacter pylori* CagA protein. Nat Rev Cancer 2004;4:688–94.

[9] Murata-Kamiya N, Kurashima Y, Teishikata Y, Yamahashi Y, Saito Y, Higashi H, et al. *Helicobacter pylori* CagA interacts with E-cadherin and deregulates the β-catenin signal that promotes intestinal transdifferentiation in gastric epithelial cells. Oncogene 2007;26:4617–26.

[10] Saadat I, Higashi H, Obuse C, Umeda M, Murata-Kamiya N, Saito Y, et al. *Helicobacter pylori* CagA targets PAR1/MARK kinase to disrupt epithelial cell polarity. Nature 2007;447:330–3.

[11] Vogelstein B, Fearon ER, Hamilton SR, Kern SE, Preisinger AC, Leppert M, et al. Genetic alterations during colorectal tumor development. N Engl J Med 1988;319:525–32.

[12] Albertson DG, Collins C, McCormick F, Gray JW. Chromosome aberrations in solid tumors. Nat Genet 2003;34:369–76.

[13] Tomioka N, Kobayashi H, Kageyama H, Ohira M, Nakamura Y, Sasaki F, et al. Chromosomes that show partial loss or gain in near-diploid tumors coincide with chromosomes that show whole loss or gain in near-triploid tumors: evidence suggesting the involvement of the same genes in the tumorigenesis of high- and low-risk neuroblastomas. Genes Chromosomes Cancer 2003;36:139–50.

[14] Houghton J, Stoicov C, Nomura S, Rogers AB, Carlson J, Li H, et al. Gastric cancer originating from bone marrow-derived cells. Science 2004;306:1568–71.

[15] Correa P, Houghton J. Carcinogenesis of *Helicobacter pylori*. Gastroenterology 2007;133:659–72.

[16] Weiss MM, Kuipers EJ, Postma C, Snijders AM, Siccama I, Pinkel D, et al. Genomic profiling of gastric cancer predicts lymph node status and survival. Oncogene 2003;22:1872–9.

[17] Tomioka N, Oba S, Ohira M, Misra A, Fridlyand J, Ishii S, et al. Novel risk stratification of patients with neuroblastoma by genomic signature, which is independent of molecular signature. Oncogene 2008;27:441–9.

[18] Pinkel D, Segraves R, Sudar D, Clark S, Poole I, Kowbel D, et al. High resolution analysis of DNA copy number variation using

comparative genomic hybridization to microarrays. Nat Genet 1998; 20:207–11.

[19] Klein CA, Schmidt-Kittler O, Schardt JA, Pantel K, Speicher MR, Riethmuller G. Comparative genomic hybridization, loss of heterozygosity, and DNA sequence analysis of single cells. Proc Natl Acad Sci U S A 1999;96:4494–9.

[20] Snijders AM, Nowak N, Segraves R, Blackwood S, Brown N, Conroy J, et al. Assembly of microarrays for genome-wide measurement of DNA copy number. Nat Genet 2001;29:263–4.

[21] Kang JU, Kang JJ, Kwon KC, Park JW, Jeong TE, Noh SM, et al. Genetic alterations in primary gastric carcinomas correlated with clinicopathological variables by array comparative genomic hybridization. J Korean Med Sci 2006;21:656–65.

[22] Do JH, Kim IS, Park TK, Choi DK. Genome-wide examination of chromosomal aberrations in neuroblastoma SH-SY5Y cells by array-based comparative genomic hybridization. Mol Cells 2007; 24:105–12.

[23] Watanabe Y, Toyota M, Kondo Y, Suzuki H, Imai T, Ohe-Toyota M, et al. PRDM5 identified as a target of epigenetic silencing in colorectal and gastric cancer. Clin Cancer Res 2007;13:4786–94.

[24] Ray ME, Wistow G, Su YA, Meltzer PS, Trent JM. *AIM1*, a novel non-lens member of the βγ-crystallin superfamily, is associated with the control of tumorigenicity in human malignant melanoma. Proc Natl Acad Sci U S A 1997;94:3229–34.

[25] Jackson A, Panayiotidis P, Foroni L. The human homologue of the *Drosophila* tailless gene (TLX): characterization and mapping to a region of common deletion in human lymphoid leukemia on chromosome 6q21. Genomics 1998;50:34–43.

[26] Yamashita T, Wada R, Sasaki T, Deng C, Bierfreund U, Sandhoff K, et al. A vital role for glycosphingolipid synthesis during development and differentiation. Proc Natl Acad Sci U S A 1999;96: 9142–7.

[27] Lang T, Hansson GC, Samuelsson T. Gel-forming mucins appeared early in metazoan evolution. Proc Natl Acad Sci U S A 2007;104: 16209–14.

[28] Zachariae W, Shin TH, Galova M, Obermaier B, Nasmyth K. Identification of subunits of the anaphase-promoting complex of *Saccharomyces cerevisiae*. Science 1996;274:1201–4.

[29] Bolognese F, Forni C, Caretti G, Frontini M, Minuzzo M, Mantovani R. The Pole3 bidirectional unit is regulated by MYC and E2Fs. Gene 2006;366:109–16.

[30] Schmucker D, Zipursky SL. Signaling downstream of Eph receptors and ephrin ligands. Cell 2001;105:701–4.

[31] Degot S, Régnier CH, Wendling C, Chenard MP, Rio MC, Tomasetto C. Metastatic lymph node 51, a novel nucleo-cytoplasmic protein overexpressed in breast cancer. Oncogene 2002;21:4422–34.

[32] Nakamura Y, Tanaka F, Nagahara H, Ieta K, Haraguchi N, Mimori K, et al. Opa interacting protein 5 (*OIP5*) is a novel cancer-testis specific gene in gastric cancer. Ann Surg Oncol 2007;14:885–92.

[33] Barre FX, Søballe B, Michel B, Aroyo M, Robertson M, Sherratt D. Circles: the replication–recombination–chromosome segregation connection. Proc Natl Acad Sci U S A 2001;98:8189–95.

[34] Wang YF, Daniel EE. Gap junctions in gastrointestinal muscle contain multiple connexins. Am J Physiol Gastrointest Liver Physiol 2001;281:G533–43.

[35] Varis A, Wolf M, Monni O, Vakkari ML, Kokkola A, Moskaluk C, et al. Targets of gene amplification and overexpression at 17q in gastric cancer. Cancer Res 2002;62:2625–9.

[36] Guo YS, Beauchamp RD, Jin GF, Townsend CM Jr, Thompson JC. Insulinlike growth factor-binding protein modulates the growth response to insulinlike growth factor 1 by human gastric cancer cells. Gastroenterology 1993;104:1595–604.

[37] Srebrow A, Friedmann Y, Ravanpay A, Daniel CW, Bissell MJ. Expression of *Hoxa-1* and *Hoxb-7* is regulated by extracellular matrix-dependent signals in mammary epithelial cells [Erratum in: J Cell Biochem 1998;71:310–312]. J Cell Biochem 1998;69: 377–91.

[38] Carè A, Felicetti F, Meccia E, Bottero L, Parenza M, Stoppacciaro A, et al. HOXB7: a key factor for tumor-associated angiogenic switch. Cancer Res 2001;61:6532–9.

[39] López R, Garrido E, Piña P, Hidalgo A, Lazos M, Ochoa R, et al. HOXB homeobox gene expression in cervical carcinoma. Int J Gynecol Cancer 2006;16:329–35.

[40] Rubin E, Wu X, Zhu T, Cheung JCY, Chen H, Lorincz A, et al. A role for the HOXB7 homeodomain protein in DNA repair. Cancer Res 2007;67:1527–35.

[41] Wang Q, Moyret-Lalle C, Couzon F, Surbiguet-Clippe C, Saurin JC, Lorca T, et al. Alterations of anaphase-promoting complex genes in human colon cancer cells. Oncogene 2003;22:1486–90.

[42] Yoo NJ, Soung YH, Lee SH, Jeong EG, Lee SH. Mutational analysis of proapoptotic integrin beta 3 cytoplasmic domain in common human cancers. Tumori 2007;93:281–3.

[43] Bouwmeester T, Bauch A, Ruffner H, Angrand PO, Bergamini G, Croughton K, et al. A physical and functional map of the human TNF-α/NF-κB signal transduction pathway [Erratum in: Nat Cell Biol 2004;6:465]. Nat Cell Biol 2004;697–105.

[44] Monteleone G, Del Vecchio Blanco G, Palmieri G, Vavassori P, Monteleone I, Colantoni A, et al. Induction and regulation of Smad7 in the gastric mucosa of patients with *Helicobacter pylori* infection. Gastroenterology 2004;126:674–82.

[45] Ngo EO, LePage GR, Thanassi JW, Meisler N, Nutter LM. Absence of pyridoxine-5′-phosphate oxidase (PNPO) activity in neoplastic cells: isolation, characterization, and expression of PNPO cDNA. Biochemistry 1998;37:7741–8.

[46] Kourmouli N, Dialynas G, Petraki C, Pyrpasopoulou A, Singh PB, Georgatos SD, et al. Binding of heterochromatin protein 1 to the nuclear envelope is regulated by a soluble form of tubulin. J Biol Chem 2001;276:13007–14.

[47] Kosco KA, Cerignoli F, Williams S, Abraham RT, Mustelin T. SKAP55 modulates T cell antigen receptor-induced activation of the Ras-Erk-AP1 pathway by binding RasGRP1. Mol Immunol 2008;45:510–22.

[48] Gu X, Zhao F, Zheng M, Fei X, Chen X, Huang S, et al. Cloning and characterization of a gene encoding the human putative ubiquitin conjugating enzyme E2Z (UBE2Z). Mol Biol Rep 2007;34: 183–8.

[49] Dohi T, Yuyama Y, Natori Y, Smith PL, Lowe JB, Oshima M. Detection of *N*-acetylgalactosaminyltransferase mRNA which determines expression of Sda blood group carbohydrate structure in human gastrointestinal mucosa and cancer. Int J Cancer 1996;67: 626–31.

[50] Li QL, Ito K, Sakakura C, Fukamachi H, Inoue K, Chi XZ, et al. Causal relationship between the loss of *RUNX3* expression and gastric cancer. Cell 2002;109:113–24.

[51] Guo WH, Weng LQ, Ito K, Chen LF, Nakanishi H, Tatematsu M, et al. Inhibition of growth of mouse gastric cancer cells by *Runx3*, a novel tumor suppressor. Oncogene 2002;21:8351–5.

[52] Brenner O, Levanon D, Negreanu V, Golubkov O, Fainaru O, Woolf E, et al. Loss of Runx3 function in leukocytes is associated with spontaneously developed colitis and gastric mucosal hyperplasia. Proc Natl Acad Sci U S A 2004;101:16016–21.

[53] Roukos DH. Innovative genomic-based model for personalized treatment of gastric cancer: integrating current standards and new technologies. Expert Rev Mol Diagn 2008;8:29–39.

Epidemiological and virological features of epidemic keratoconjunctivitis due to new human adenovirus type 54 in Japan

Hisatoshi Kaneko,[1] Tatsuo Suzutani,[1] Koki Aoki,[2] Nobuyoshi Kitaichi,[2] Susumu Ishida,[2] Hiroaki Ishiko,[3] Tsutomu Ohashi,[4] Shigeki Okamoto,[5] Hisashi Nakagawa,[6] Rikutaro Hinokuma,[7] Yoshimori Asato,[8] Shinobu Oniki,[9] Teiko Hashimoto,[10] Tomohiro Iida,[11] Shigeaki Ohno[12]

[1]Department of Microbiology, Fukushima Medical University School of Medicine, Fukushima, Japan
[2]Department of Ophthalmology, Hokkaido University Graduate School of Medicine, Sapporo, Japan
[3]Host Defense Laboratory, Mitsubishi Chemical Medience Corporation, Tokyo, Japan
[4]Ohashi Eye Clinic, Sapporo Japan
[5]Okamoto Eye Clinic, Matsuyama, Japan
[6]Tokushima Eye Clinic, Tokyo, Japan
[7]Hinokuma Eye Clinic, Kumamoto, Japan
[8]Asato Eye Clinic, Itoman, Japan
[9]Oniki Eye Clinic, Chikushino, Japan
[10]Sakuramizu Sakai Eye Clinic, Fukushima, Japan
[11]Department of Ophthalmology, Fukushima Medical University School of Medicine, Fukushima, Japan
[12]Department of Ocular Inflammation and Immunology, Hokkaido University Graduate School of Medicine, Sapporo, Japan

Correspondence to
Dr Hisatoshi Kaneko, Department of Microbiology, Fukushima Medical University School of Medicine, 1 Hikarigaoka, Fukushima 960-1295, Japan; h-kane@chive.ocn.ne.jp

Accepted 20 March 2010
Published Online First 8 June 2010

ABSTRACT

Background/aims New human adenovirus (HAdV)-54 causes epidemic keratoconjunctivitis (EKC) and is virologically close to and has occasionally been detected as HAdV-8. Taking HAdV-54 into account, we re-determined HAdV type in EKC samples to determine its epidemiology in Japan, and examined the virological features of HAdV-54.

Methods HAdV type was re-determined in 776 conjunctival swabs from Japan and 174 from six other countries, obtained between 2000 and 2009. Using 115 HAdV strains obtained before 1999, trends regarding HAdV-8 and HAdV-54 were also determined. In addition, immunochromatography (IC) kit features, DNA copy numbers and viral isolation of HAdV-54 in samples were evaluated.

Results Recently, HAdV-37 and HAdV-54 have been the major causative types of EKC in Japan. HAdV-54 has been isolated each year since 1995, whereas HAdV-8 has become less common since 1997, although it remains the most common cause of EKC in the six other countries investigated where HAdV-54 is yet to be detected. HAdV-54 is comparable to other EKC-related HAdV types in terms of IC kit sensitivity and DNA copy numbers, although HAdV-54 grows more slowly on viral isolation.

Conclusions EKC due to HAdV-54 can result in epidemics; therefore, it should be accurately diagnosed and monitored as an emerging infection worldwide.

INTRODUCTION

Epidemic keratoconjunctivitis (EKC) is a contagious conjunctivitis associated with community-acquired infection.[1 2] In Japan, EKC affects approximately 1 million patients annually and epidemics are carefully monitored by the National Surveillance Center. Moreover, nosocomial EKC infections often occur, resulting in severe outbreaks in ophthalmology wards and necessitating the restriction of clinical practices, such as the postponement of eye surgery, the early release of inpatients from hospital and the closure of ophthalmology wards. These restrictions may also have an economic impact on medical institutions involved; therefore, nosocomial infection has become a serious social problem in Japan.[3 4]

EKC is caused by human adenovirus (HAdV). HAdVs belong to the genus Mastadenovirus of the family Adenoviridae and are classified into seven species, A to G (HAdV-A to HAdV-G).[2 5] Adenoviral conjunctivitis is mainly caused by HAdV-3 (in HAdV-B), HAdV-4 (in HAdV-E), and HAdV-8, HAdV-19a and HAdV-37 (in HAdV-D). Among these, HAdV-4, HAdV-8, HAdV-19a and HAdV-37 are known to cause EKC. Recently, two new HAdV types that cause EKC were identified and named HAdV-53 and HAdV-54.[6–9] HAdV-54 was first isolated from a nosocomial EKC infection in Japan in 2000, and was reported as a novel HAdV serotype on the basis of neutralisation tests (NT) and the low identity of the nucleotide sequences in hexon loop one and two, which contain the NT epitope, compared with all other HAdV types.[6] Thereafter, this strain was numbered HAdV-54 from the analysis of the complete genome sequence.[9 10] Since 2000, HAdV-54 has often caused EKC in Japan, but it has not yet been isolated in countries other than Japan. HAdV-54 was found to be weakly reactive to HAdV-8 antiserum by NT and the nucleotide sequence of the genome appeared similar to that of HAdV-8.[6 9] Therefore, it has occasionally been detected as HAdV-8.[9] In brief, taking HAdV-54 into account, we re-typed conjunctival samples from EKC patients obtained after 2000 by phylogenetic analyses of the partial hexon sequences. As a result, we found that most HAdV-54 strains had been mistyped as HAdV-8, suggesting that HAdV-54 might have caused EKC before 2000 in Japan and more recently in other countries.

To prevent outbreaks, ophthalmologists require a rapid and accurate diagnostic test, and the detection of HAdV from conjunctival swabs by methods such as immunochromatography (IC) kit, PCR and viral isolation are extremely useful for the diagnosis of EKC. However, detection by these methods depends on the viral load in the samples. Moreover, the sensitivity of IC kits and growth speed of HAdV varies between HAdV type.[11] Currently, the detailed virological features of HAdV-54 remain unknown.

In this study, taking the possible mistyping of HAdV-54 into account, we re-determined the HAdV type in clinical samples obtained from EKC patients between 2000 and 2009 in Japan to determine the exact epidemiology of EKC in Japan. This was then compared with the epidemiology of EKC in six other countries. In addition, we re-typed HAdV strains that were identified as HAdV-8 by

NT between 1990 and 1999, and determined the trends regarding these two HAdV types. Moreover, the virological features of HAdV-54 were compared with those of other EKC-related HAdV types.

MATERIALS AND METHODS

Sample collection from EKC patients between 2000 and 2009

We collected 776 conjunctival swabs for DNA analysis from patients with EKC in Japan and 174 from other countries between 2000 and 2009. Among the samples obtained in Japan, 573 swabs were collected from nine eye clinics treating cases of sporadic infection, and the other 203 samples were from 29 medical institutions that treated outbreaks of nosocomial infection in different parts of Japan. The 174 swabs obtained outside Japan were collected from cases of sporadic infection in six countries: 12 swabs from the USA, 28 from Saudi Arabia, 30 from Nepal, 12 from Vietnam, 10 from Bangladesh and 82 from Austria. The samples were scraped from the lower palpebral conjunctiva using a cotton swab and stored at −80°C until use.

HAdV strains detected as HAdV-8 between 1990 and 1999

To determine when HAdV-54 first appeared, as well as delineate the transition from HAdV-8 to HAdV-54, a total of 115 HAdV strains, which were identified as HAdV-8, were collected in Japan between 1990 and 1999. All strains were identified as HAdV-8 by NT with serotype-specific antiserum purchased from the American Type Culture Collection (Manassas, VA, USA).

DNA extraction

Viral DNA was extracted from 100 µl of each virus solution or eye swab using a Sumitest EX-R&D kit (Medical & Biological Laboratories, Nagano, Japan) according to the manufacturer's instructions. The extracted DNA was then suspended in 100 µl of Tris/EDTA (TE) buffer (10 mM Tris, 1 mM EDTA, pH 8.0).

Phylogeny-based classification for HAdV typing

For HAdV typing, nucleotide sequences in the partial hexon were amplified and subjected to phylogenetic analysis as described previously.[12] The nucleotide sequences of the PCR products were determined using a CEQ 2000XL DNA analysis system with a DyeTerminator cycle sequencing kit (Beckman Coulter, Fullerton, California, USA) and compared with those of all 52 serotypes and HAdV-54 using SINCA (Fujitsu Limited, Tokyo, Japan). HAdV-53, a novel recombinant HAdV, was clustered with HAdV-37 according to the above phylogenetic analysis. For the typing of HAdV-37 and HAdV-53, the nucleotide sequences in the fibre knob was amplified and subjected to phylogenetic analysis as described previously.[7] HAdV-37 and HAdV-53 formed clusters with HAdV-37 and HAdV-8 prototypes, respectively. The evolutionary distances were estimated using Kimura's two-parameter method,[13] and unrooted phylogenetic trees were constructed using the neighbour-joining method.[14] Bootstrap analyses were performed with 1000 resamplings of the data sets.[15]

Detection of HAdV antigen by IC kit

Adenocheck IC kits (Santen Pharmaceutical, Osaka, Japan)[11] were used in this study. Among the sporadic samples from Japan, 70 samples were used for the IC kit evaluation. Conjunctival swabs were extracted with 500 µl of mucolytic agent provided by the manufacturer. An aliquot of the extract (200 µl) was filtered and dropped into the IC kit device. Both the test-tube and filter were provided by the manufacturer. The IC kit indicated a positive result when two lines appeared in the device. When only one line appeared in the control area of the IC kit, the result was considered to be negative.

Detection and quantitation of HAdV DNA by real-time PCR

HAdV DNA copy numbers in samples were quantified by real-time PCR using ABI PRISM 7000 (Foster City, USA) as described previously.[12] The detection limit of this real-time PCR was 10 copies/µl.

Viral isolation

Among the sporadic samples from Japan, 102 samples were used for viral isolation. Swabs for viral isolation were placed in 0.5 ml of Dulbecco's Modified Eagle Medium (DMEM) (Life Technologies, Rockville, Maryland, USA) and stored at −80°C until use. Swab solution (100 µl) was added to A549 cells and incubated at 37°C. Cell cultures were maintained in DMEM containing 50 µg/ml of gentamicin, 0.5 µg/ml of fungizone and 10% fetal calf serum. The cultures were observed daily for the cytopathic effects (CPEs) of HAdV for up to 35 days with blind passage. The blind passage was carried out once per week. When no CPE was observed by the fourth blind passage, the cultures were considered to be CPE-negative.

Statistical analysis

Statistical significance was evaluated with Student t test and $p<0.05$ was considered significant.

RESULTS

Phylogeny-based classification of samples collected from sporadic infection cases in seven countries

HAdV DNA was detected by PCR from all 573 and 174 sporadic infection samples obtained in Japan and other countries, respectively. The relative proportions of HAdV types for each country are shown in figure 1. Among the samples obtained in Japan, 40, 19, 19, 270, 66 and 159 swabs were identified as HAdV-4, HAdV-8, HAdV-19a, HAdV37, HAdV-53 and HAdV-54, respectively. The main causative types of EKC were HAdV-37

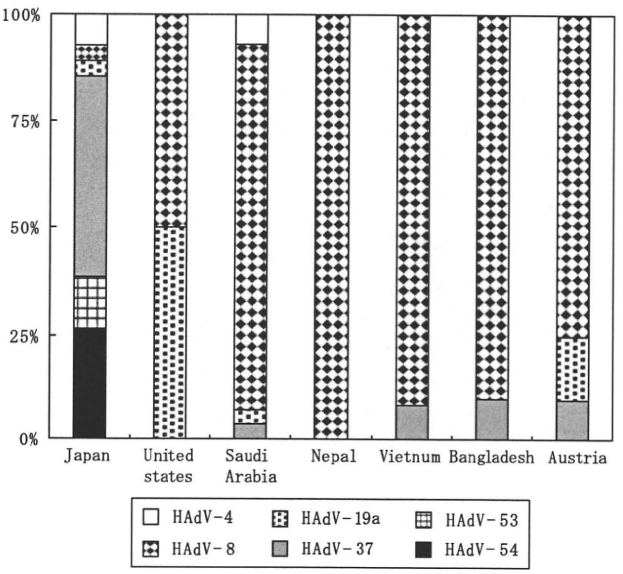

Figure 1 The relative proportions of human adenovirus (HAdV) types isolated from conjunctival swabs from patients with sporadic epidemic keratoconjunctivitis (EKC) obtained between 2000 and 2009 in Japan, the USA, Saudi Arabia, Nepal, Vietnam, Bangladesh and Austria.

and HAdV-54. The number of samples containing HAdV-8, the original agent for EKC, was low in Japan. On the other hand, among the samples obtained in the other six countries, 139 of the 174 samples were identified as HAdV-8, and HAdV-8 was the major causative agent for EKC in all six countries. No HAdV-53 or HAdV-54 strains were identified.

HAdV types in nosocomial infections in Japan

HAdV DNA was detected by PCR from all 203 samples from 29 medical institutions treating outbreaks of nosocomial EKC infection. All samples from each individual medical institution showed an identical HAdV type. HAdV-4, HAdV-19a, HAdV37, HAdV-53 and HAdV-54 were the causative HAdV types of nosocomial infection in two, two, twelve, four and nine institutions, respectively (figure 2). The relative proportions of HAdV types causing nosocomial infection in each institution are shown in figure 2. HAdV-37 and HAdV-54 frequently caused nosocomial infections in Japan, but no nosocomial infections were caused by HAdV-8.

The trends for HAdV-8 and HAdV-54 between 1990 and 2009 in Japan

Among the 115 HAdV strains obtained between 1990 and 1999, 85 were identified as HAdV-8 and 30 as HAdV-54. In addition to the 88 samples of sporadic infection obtained between 2000 and 2009, we determined the trends for these two HAdV types between 1990 and 2009. The numbers of HAdV-8 and HAdV-54 strains isolated for every 5-year period are shown in figure 3. During the initial 5-year period, every sample was identified as HAdV-8. However, HAdV-8 has become far less common since 1997: only one strain was isolated in 2001 and three in 2003. Finally, no HAdV-8 strains have been detected since 2004. In contrast, HAdV-54 was first identified from 12 samples in 1995, and has been detected each year since then. During the first and second 5-year periods (1990–1999), 30 samples of HAdV-54 had been mistyped as HAdV-8. Seventy-six of the 80 samples (95.5%) obtained from 2000–2009 were HAdV-54-positive.

IC kit sensitivity and quantitation of HAdV DNA

Among the 70 samples tested, 36 and 46 were found to be IC kit- and PCR-positive, respectively. Of the 46 PCR-positive samples, eight contained HAdV-3, 22 contained HAdV-37 and 16 contained HAdV-54 according to the phylogeny-based classification of PCR products in the partial hexon gene.[12] Among these PCR-positive samples, 36 and 10 were IC kit-positive and

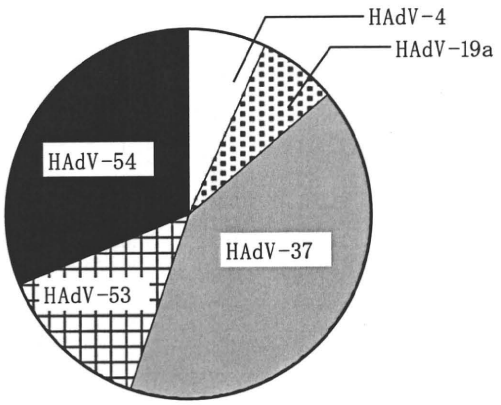

Figure 2 The relative proportions of human adenovirus (HAdV) types isolated from samples from cases of nosocomial infection obtained from medical institutions between 2000 and 2009 in Japan.

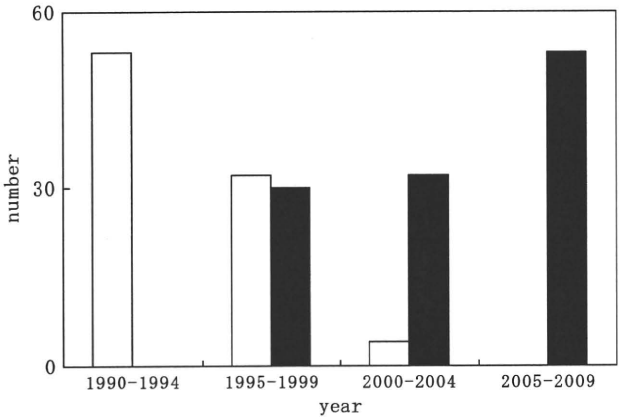

Figure 3 The trends for human adenovirus (HAdV)-8 (white bars) and HAdV-54 (black bars) for every 5-year period from 1990 to 2009 in Japan.

-negative, respectively. All PCR-negative samples were also IC-kit negative. The sensitivity of the IC kits and DNA copy numbers for each HAdV type are shown in table 1. The IC kit sensitivity for each HAdV type was calculated as the number of IC kit-positive samples/the number of real-time PCR-positive samples. There were no statistically differences in IC kit sensitivity or copy number between HAdV-3, HAdV-37 and HAdV-54.

The observation of CPE during viral isolation

CPEs were observed during tissue culture in 68 of the 102 samples. Among these samples, HAdV-3, HAdV-4, HAdV-19a, HAdV-37 and HAdV-54 were identified in five, four, five, 41 and 13 samples, respectively, by phylogeny-based classification.[12] No HAdV-8 was detected. CPEs were observed in 44 of 68 samples (66.7%) during primary culture, in 18 samples (27.3%) during first passage, in two samples (3.0%) during second passage, and in two samples (3.0%) during third passage. No CPE was observed during the fourth passage. All samples containing HAdV-3, HAdV-4 and HAdV-19 showed CPEs during primary tissue culture. Blind passage was required for 37% of samples containing HAdV-37 and 64% containing HAdV-54 strains. On average, the CPE was detected at 4.4 days for HAdV-3, 7.0 days for HAdV-4, 4.8 days for HAdV-19, 9.0 days for HAdV-37, and 11.5 days for HAdV-54. Statistically significant differences were shown between HAdV-54 and HAdV-3, HAdV-19 and HAdV-37, and between HAdV-37 and HAdV-3 (figure 4).

DISCUSSION

Since HAdV-54 was first reported in 2000 in Japan, the incidences of sporadic and nosocomial EKC due to HAdV-54 were 26.3% and 31.0%, respectively; together with HAdV-37, HAdV-54 has recently been the main cause of EKC in Japan. HAdV-54 had caused EKC in 1995, but it was mistyped as HAdV-8 in the 1990s. Since 1995, a number of cases of EKC

Table 1 HAdV DNA copy numbers and sensitivity of IC kit for EKC samples

HAdV type	No. of samples	No. of copies/μl			Sensitivity of IC kit (%)
		Minimum	Maximum	Mean	
HAdV-3	8	1.52×10^3	4.26×10^8	2.05×10^7	75.0
HAdV-37	22	1.07×10^3	2.27×10^8	3.95×10^7	81.8
HAdV-54	16	2.77×10^3	1.98×10^9	1.41×10^8	81.2

EKC, epidemic keratoconjunctivitis; HAdV, human adenovirus; IC, immunochromatography.

Br J Ophthalmol 2011;**95**:32–36. doi:10.1136/bjo.2009.178772

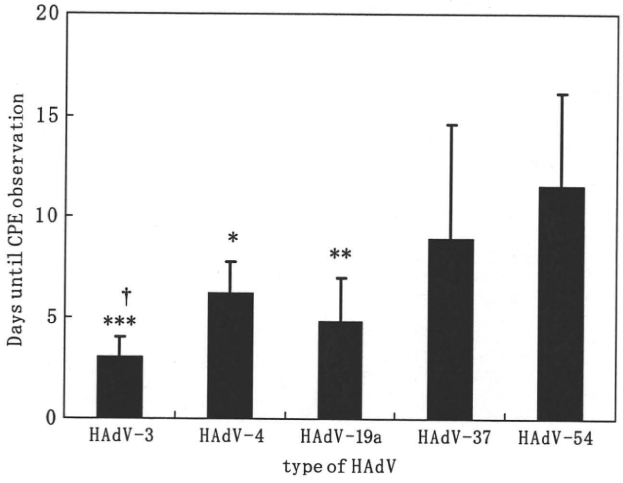

Figure 4 Number of days until observation of cytopathic effects (CPE) in human adenoviruses (HAdVs) causing epidemic keratoconjunctivitis (EKC). The results are expressed as means±SD (error bars). Significant differences compared with HAdV-54: *p<0.05; **p<0.01; ***p<0.001. Significant differences compared with HAdV-37: †p<0.05.

have been caused by HAdV-54 each year. Interestingly, as the incidence of EKC due to HAdV-54 has increased, that due to HAdV-8 has fallen. HAdV-8 was first isolated in 1955 and has been regarded as the original causative agent of EKC.[16] Thereafter, HAdV-19a and HAdV-37 were found as causative agents of EKC,[17 18] but HAdV-8 remained the predominant HAdV serotype isolated in association with EKC in many countries.[3 19–22] In this study, HAdV-8 was seen to commonly still cause EKC in the six other countries investigated. Originally, not only HAdV-8, but also HAdV-4, HAdV-19a and HAdV-37, were often isolated from patients with EKC in Japan. Due to the occurrence of multiple HAdV types, the incidence of EKC might be much higher than in other countries and outbreaks were common. EKC outbreaks due the onset of new genome types or in which nucleotide polymorphisms were observed in the genome of the responsible HAdV type have been reported.[23 24] Moreover, intermediate HAdV types produced by recombination between different HAdV types have also led to EKC epidemics.[7 8] Outbreaks due to these genomic variations, substitutions and recombinations might result in the appearance of new HAdV types. HAdV-54 was found to be close to the HAdV-8 strain over the entire genome[6 10]; therefore, HAdV-54 might have evolved from HAdV-8, and the incidence of HAdV-8 might have fallen due to this evolutionary change.

HAdV-54 was not identified in any of the six countries studied except Japan. However, HAdV-54 might cause EKC epidemic worldwide in the future. The HAdV typing from clinical samples, particularly ocular samples, is necessary as HAdV-54 cannot be detected by NT because of an absence of serotype-specific antiserum. Currently, phylogeny-based classification using the partial hexon gene is the only method for the detection of HAdV-54.[6 12] A standard method for the detection of HAdV-54 should be established and made public as soon as possible.

HAdV-3-, HAdV-37- and HAdV-54-positive samples showed the almost same HAdV copy numbers and IC kit sensitivities. As we previously reported, similar results were obtained for other EKC-related HAdV types (HAdV-4, HAdV-8 and HAdV-19a),[4 11] indicating that HAdV-54 could be detected by conventional IC kits and/or PCR systems. However, HAdV-54 requires a longer period until the appearance of CPEs and is slower growing than HAdV-3, HAdV-4, HAdV-19a and HAdV-37 during viral isolation. HAdV-8 could not be isolated in this study, and it is also known to be slow growing, requiring a number of passages during viral isolation.[25] Thus, suspected EKC samples should be cultured as long as possible and with multiple blind passages for the isolation of HAdVs.

In conclusion, the new HAdV-54 type is likely to be the cause of EKC epidemics and should be monitored worldwide as an emerging virus. Moreover, the evolution of and mutations in the HAdV genome might lead to the appearance of other new HAdV types and further outbreaks of EKC. EKC-related HAdVs should, therefore, be carefully monitored in the future.

Acknowledgements We thank Prof. KF Tabbara (The Eye Center and The Eye Foundation for Research in Ophthalmology), Prof. F Huq (Chittagong Infirmary & Training Complex/Institute), Prof. YJ Gordon (University of Pittsburgh) and Dr M Nagl (University of Innsbruck) for supplying the materials used in this study.

Competing interests None.

Patient consent Obtained.

Provenance and peer review Not commissioned; externally peer reviewed.

REFERENCES

1. **Swenson PD,** Wadell G, Allard A, *et al*. Adenoviruses. In: Murray E, Baron J, Pfaller MA, *et al*, eds. *Manual of clinical microbiology*. 8th edn. **vol. 2**. Washington, DC: ASM Press, 2003:1404–17.
2. **Benkö M,** Harrach B, Russell WC. Family adenoviridae. In: van Regenmortel MHV, Fauquet CM, Bishop DHL, *et al*, eds. *Virus taxonomy: seventh report of the international committee on taxonomy of viruses*. San Diego: Academic Press, 2000:227–38.
3. **Aoki K,** Tagawa Y. A twenty-one year surveillance of adenoviral conjunctivitis in Sapporo, Japan. *Int Ophthalmol Clin* 2002;**42**:49–54.
4. **Kaneko H,** Maruko I, Iida T, *et al*. The possibility of human adenovirus detection from the conjunctiva in asymptomatic cases during nosocomial infection. *Cornea* 2008;**27**:527–30.
5. **Jones MS,** Harrach B, Ganac RD, *et al*. New adenovirus species found in a patient presenting with gastroenteritis. *J Virol* 2007;**81**:5978–84.
6. **Ishiko H,** Shimada Y, Konno T, *et al*. A novel human adenovirus causing nosocomial infections of epidemic keratoconjunctivitis. *J Clin Microbiol* 2008;**46**:2002–8.
7. **Aoki K,** Ishiko H, Konno T, *et al*. Epidemic keratoconjunctivitis due to the novel hexon-chimeric-intermediate 22,37/H8 human adenovirus. *J Clin Microbiol* 2008;**46**:3259–69.
8. **Walsh MP,** Chintakuntlawar A, Robinson CM, *et al*. Evidence of molecular evolution driven by recombination events influencing tropism in a novel human adenovirus that causes epidemic keratoconjunctivitis. *PLoS One* 2009;**4**:e5635.
9. **Ishiko H,** Aoki K. Spread of epidemic keratoconjunctivitis due to a novel serotype of human adenovirus in Japan. *J Clin Microbiol* 2009;**47**:2678–9.
10. **Kaneko H,** Iida T, Ishiko H, *et al*. Analysis of the complete genome sequence of epidemic keratoconjunctivitis-related human adenovirus type 8, 19, 37 and a novel serotype. *J Gen Virol* 2009;**90**:1471–6.
11. **Uchio E,** Aoki K, Saitoh W, *et al*. Rapid diagnosis of adenoviral conjunctivitis on conjunctival swabs by 10-minute immunochromatography. *Ophthalmology* 1997;**104**:1294–9.
12. **Miura-Ochiai R,** Shimada Y, Konno T, *et al*. Quantitative detection and rapid identification of human adenoviruses. *J Clin Microbiol* 2007;**45**:958–67.
13. **Kimura M.** A simple method for estimating evolutionary rates of base substitutions through comparative studies of nucleotide sequence. *J Mol Evol* 1980;**16**:111–20.
14. **Saitou N,** Nei M. The neighbor-joining method: a new method for reconstructing phylogenetic trees. *Mol Biol Evol* 1987;**4**:406–25.
15. **Felsenstein J.** Confidence limits on phylogenies: an approach using the bootstrap. *Evolution* 1985;**39**:783–91.
16. **Jawetz E,** Hanna L, Thygeson PA. Laboratory infection with Ad8. *Am J Hyg* 1959;**69**:13–20.
17. **Wadell G,** De Jong JC. Restriction endonucleases in identification of a genome type of adenovirus 19 associated with keratoconjunctivitis. *Infect Immun* 1980;**27**:292–6.
18. **De Jong JC,** Wigand R, Wadell G, *et al*. Adenovirus 37: identification and characterization of a medically important new adenovirus type of subgroup D. *J Med Virol* 1981;**7**:105–18.
19. **Ishii K,** Nakazono N, Fujinaga K, *et al*. Comparative studies on aetiology and epidemiology of viral conjunctivitis in three countries of East Asia — Japan, Taiwan and South Korea. *Int J Epidemiol* 1987;**16**:98–103.

20. **Vainio K,** Borch E, Bruu AL. No sequence variation in part of the hexon and the fibre genes of adenovirus 8 isolated from patients with conjunctivitis or epidemic keratoconjunctivitis (EKC) in Norway during 1989 to 1996. *J Clin Pathol* 2001;**54**:558–61.
21. **Jin XH,** Ishiko H, Nguyen TH, *et al*. Molecular epidemiology of adenoviral conjunctivitis in Hanoi, Vietnam. *Am J Ophthalmol* 2006;**142**:1064–6.
22. **Higuchi M,** Nakazono N, Ishii K, *et al*. Antigenic and restriction endonuclease analyses of new adenovirus types 19 and 37 causing acute conjunctivitis. *Jpn J Ophthalmol* 1987;**31**:547–57.
23. **Ariga T,** Shimada Y, Shiratori K, *et al*. Five new genome types of adenovirus type 37 caused epidemic keratoconjunctivitis in Sapporo, Japan, for more than 10 years. *J Clin Microbiol* 2005;**43**:726–32.
24. **Kaneko H,** Iida T, Ohguchi T, *et al*. Nucleotide sequence variation in the hexon gene of human adenovirus type 8 and 37 strains from epidemic keratoconjunctivitis patients in Japan. *J Gen Virol* 2009;**90**:2260–5.
25. **Saitoh-Inagawa W,** Oshima A, Aoki K, *et al*. Rapid diagnosis of adenoviral conjunctivitis by PCR and restriction fragment length polymorphism analysis. *J Clin Microbiol* 1996;**34**:2113–16.

Cover illustration

Smoky solution to pressure problems: Fick's Ophthalmotonometer

That raised eye pressure can damage the eye and affect vision was known long before a method to measure eye pressure was devised. The first attempt to measure the intraocular pressure was by Albrecht von Graefe in 1862. In 1857 he had introduced the 'Iridectomy' operation, the first effective surgical treatment of glaucoma, for the relief of pressure in the eye and wanted to determine the pre- and postoperative eye pressure measurements to assess the effect of his operations. His experimental impression tonometer was not a success nor were a number of subsequent instruments designed by Frans Donders who was the first to use the term ophthalmotonometer in 1863. Hermann Snellen, Henri Dor and others were also unsuccessful. The first impression tonometer for general use, which worked by indenting a part of the globe, was invented by Hjalmar Schiotz in 1905.

In 1888, Adolf Fick introduced a tonometer that used a spring action with a flat plate applied to the temporal sclera (figure 1). The pressure in the spring varied according to the applanation of the plate. Apart from the inherent inaccuracies of this method the observer had difficulty in knowing when the plate was applanted on the sclera. F Oswalt, a French ophthalmologist, recognised the difficulty of viewing the plate at the same time as reading the deflection on the scale. He devised a rather unusual solution comprised of a triangular shaped piece of glass that was smoked and placed behind a scraper, which was attached to the lever extending from the plate (figure 2). When applanation had been achieved a thin line was scratched into the smoke deposit on the glass terminating at a point in line with the pressure marked on the scale. The instrument shown on the cover illustrates this modified Fick's tonometer. The instrument was made by Charles Verdin of Paris.

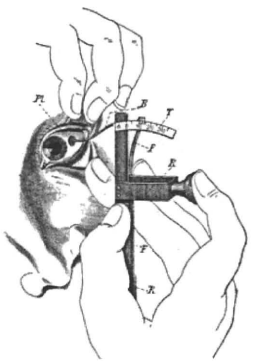

Figure 1 The Fick ophthalmotonometer which was used to applanate the sclera to measure intraocular pressure.

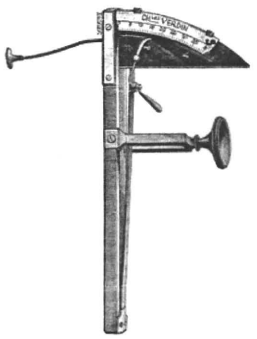

Figure 2 The Fick Oswalt ophthalmotonometer where a smoked glass plate was incorporated to facilitate reading of the pressure value.

Adolf Fick (1829–1901) was a physiologist, born in Kassel and is perhaps best known for Fick's Law for the diffusion of matter, proposed in 1855. He held the Chair of Physiology at the University of Zurich in 1856 and then moved to Wurzburg where he held the Chair of Physiology until 1898. He is not to be confused with his nephew of the same name, Adolf Eugen Fick, who invented the contact lens.

The name Fick (the uncle Fick but referenced as Fick RA in some publications),[1 2] is also intimately tied in with the 'Imbert-Fick law' which states that 'the pressure (T) inside a sphere filled with liquid and surrounded by an infinitely thin membrane can be measured by the counter pressure (P) which just flattens the membrane. The law presupposes that the membrane is without rigidity and elasticity: T=P/A (A is a constant)'.[3] It is contended that this is not really a 'law' but was 'invented by Hans Goldmann (1899–1991) to give his newly marketed tonometer (with the help of the Haag-Streit Company) a quasi scientific basis; it is mentioned in the ophthalmic and optometric literature, but not in any books of physics'.[3 4]

Richard Keeler, Arun D Singh, Harminder S Dua

Provenance and peer review Not commissioned; not externally peer reviewed.

Br J Ophthalmol 2011;**95**:36. doi:10.1136/bjo.2010.199588

REFERENCES

1. **Fick RA.** Ein neues ophthalmotonometer. *Verhandlungen derPhysikalisch-Medizinische Gesellshaft Zu Würzburg* 1888;**22**:151.
2. **Stuckey GC.** Application of physical principles in the development of tonometry. *Clinical Exp Ophthalmol* 2004;**32**:633–6.
3. **Markiewitz HH.** The so-called Imbert-Fick Law. *AMA Arch Ophthalmol* 1960;**64**:189–59.
4. **http://en.wikipedia.org/wiki/Imbert-Fick_law** (accessed 16 Nov 2010).

Experimental Eye Research 90 (2010) 41–48

Contents lists available at ScienceDirect

Experimental Eye Research

journal homepage: www.elsevier.com/locate/yexer

Prevention of experimental autoimmune uveoretinitis by blockade of osteopontin with small interfering RNA☆

Daiju Iwata [a,b], Mizuki Kitamura [a,b], Nobuyoshi Kitaichi [b], Yoshinari Saito [c], Shigeyuki Kon [c], Kenichi Namba [b], Junko Morimoto [c], Akiko Ebihara [a,b], Hirokuni Kitamei [b], Kazuhiko Yoshida [b], Susumu Ishida [b], Shigeaki Ohno [d], Toshimitsu Uede [c], Kazunori Onoé [a], Kazuya Iwabuchi [a,d,*]

[a] Division of Immunobiology, Institute for Genetic Medicine, Hokkaido University, Kita-15, Nishi-7, Kita-ku, Sapporo 060-0815, Japan
[b] Department of Ophthalmology and Visual Sciences, Hokkaido University Graduate School of Medicine, Sapporo, Japan
[c] Division of Molecular Immunology, Institute for Genetic Medicine, Hokkaido University, Sapporo, Japan
[d] Department of Ocular Inflammation and Immunology, Hokkaido University Graduate School of Medicine, Sapporo, Japan

ARTICLE INFO

Article history:
Received 16 July 2008
Accepted in revised form
9 September 2009
Available online 18 September 2009

Keywords:
inflammation
EAU
OPN
RNA interference
uveitis

ABSTRACT

Osteopontin (OPN) is elevated during the progression of experimental autoimmune uveoretinitis (EAU) in C57BL/6 (B6) mice. Furthermore, EAU symptoms are ameliorated in OPN knockout mice or in B6 mice treated with anti-OPN antibody (M5). Recently, OPN has been shown to promote the Th1 response not only in the extracellular space as a secretory protein but also in cytosol as a signaling component. Thus, we attempted to reduce OPN in both compartments by using a small interfering RNA (siRNA) targeting the OPN coding sequence (OPN-siRNA). EAU was induced in B6 mice by immunization with human interphotoreceptor retinoid-binding protein (hIRBP) peptide sequence 1–20. The OPN- or control-siRNA was administered with hydrodynamic methods 24 h before and simultaneously with immunization (prevention regimen). When plasma OPN levels were quantified following siRNA administration with the prevention regimen, the level in the OPN-siRNA-treated group was significantly lower than that in the control-siRNA-treated group. Accordingly, the clinical and histopathological scores of EAU were significantly reduced in B6 mice when siRNA caused OPN blockade. Furthermore, TNF-α, IFN-γ, IL-2, GM-CSF and IL-17 levels in the culture supernatants were markedly suppressed in the OPN-siRNA-treated group, whereas the proliferative responses of T lymphocytes from regional lymph nodes against immunogenic peptides was not significantly reduced. On the other hand, the protection was not significant if the mice received the OPN-siRNA treatment on day 7 and day 8 after immunization when the clinical symptoms appeared overt (reversal regimen). Our results suggest that OPN blockade with OPN-siRNA can be an alternative choice for the usage of anti-OPN antibody and controlling uveoretinitis in the preventive regimen.

1. Introduction

Experimental autoimmune uveoretinitis (EAU) is an animal model of human endogenous uveoretinitis, including sympathetic ophthalmia, birdshot retinochoroidopathy, Vogt-Koyanagi-Harada's disease, and Behçet's disease (Caspi et al., 1988). EAU is induced by immunization with a retinal antigen (Ag), e.g., interphotoreceptor retinoid-binding protein (IRBP), or by the adoptive transfer of retinal Ag-specific T lymphocytes (Mochizuki et al., 1985; Caspi et al., 1986; Gregerson et al., 1986). EAU induced with immunization of retinal Ag now represents not only Th1 but also Th17-cell-mediated ocular diseases. A massive inflammatory infiltration composed primarily of mononuclear cells causes a rapid and irreversible destruction of photoreceptor cells (Jiang et al., 1999; Silver et al., 1999; Caspi, 2003; Amadi-Obi et al., 2007; Luger et al., 2008). It has been demonstrated that the augmentation of the Th2 response and T regulatory cytokine production and down-regulation of the Th1 response can mitigate inflammation and protect against the development of EAU (Saoudi et al., 1993; Kezuka et al., 1996; Caspi, 2002).

☆ This work was supported in part by a grant for Research on Behçet's Disease from The Ministry of Health, Labor, and Welfare Japan, by Grants-in-Aid for Scientific Research (S) and (C) from the Japan Society for the Promotion of Science (JSPS) and a Grant-in-Aid for Scientific Research on Priority Areas from The Ministry of Education, Culture, Sports, Science and Technology (MEXT) Japan. KI is also supported by the Global COE Program 'Establishment of International Collaboration Center for Zoonosis Control' from MEXT, and grants from The Suhara Memorial Foundation and Heisei Ijuku Tomakomai East Hospital.

* Corresponding author at: Division of Immunobiology, Institute for Genetic Medicine, Hokkaido University, Kita-15, Nishi-7, Kita-ku, Sapporo 060-0815, Japan. Tel.: +81 11 706 5532; fax: +81 11 706 7545.
E-mail address: akimari@igm.hokudai.ac.jp (K. Iwabuchi).

0014-4835/$ – see front matter © 2009 Elsevier Ltd. All rights reserved.
doi:10.1016/j.exer.2009.09.008

Osteopontin (OPN), also known as early T lymphocyte activation 1 (Eta-1), a secreted phosphoglycoprotein (SPP), contains the arginine-glycine-aspartic acid (RGD) integrin-binding sequence that is found in many extracellular matrix (ECM) proteins (O'Regan and Berman, 2000). OPN mediates adhesion and migration of a number of different cells types (O'Regan and Berman, 2000). OPN is widely produced by a variety of inflammatory cells, including T cells, macrophages, NK cells, and NKT cells (Denhardt et al., 2001; Diao et al., 2004, 2008) and induces interleukin-12 (IL-12) and IFN-γ production and inhibits IL-10 expression (Ashkar et al., 2000). Moreover, the intracellular isoform, OPN-i is now considered to promote the Th1 response through type I interferon production (Shinohara et al., 2006; Cantor and Shinohara, 2009). OPN has therefore been considered to act as a cytokine contributing to the development of Th1-mediated immunity and diseases and is anticipated to be a therapeutic target for controlling these diseases.

Indeed, recent studies, including ours, indicate that OPN possesses an aggravating role in EAU (Hikita et al., 2006; Kitamura et al., 2007), as had already been demonstrated in experimental autoimmune encephalomyelitis (EAE) (Ashkar et al., 2000; Chabas et al., 2001), anti-type II collagen antibody-induced arthritis (Yumoto et al., 2002; Yamamoto et al., 2003), and autoimmune hepatitis (Diao et al., 2004; Saito et al., 2007). Furthermore, we demonstrated that a specific antibody (M5) reacting to the SLAYGLR sequence, a newly exposed binding site, within OPN by thrombin cleavage, significantly suppressed clinical and histopathological scores of EAU in mice (Kitamura et al., 2007).

RNA interference (RNAi) is a powerful tool for silencing gene expression, by which double-stranded RNA (dsRNA) triggers the sequence-specific degradation of messenger RNA. In particular, small interfering RNAs (siRNAs), 21–23 nucleotide-length fragments (Elbashir et al., 2001; Hannon, 2002; Xie et al., 2006), have been shown to be of great value in decreasing the expression of the target gene by *in vivo* administration (Song et al., 2003; Nakamura et al., 2004; Schiffelers et al., 2005; Khoury et al., 2006).

In the present study, we applied siRNA targeting to an OPN coding sequence (OPN-siRNA) to inhibit OPN function by reducing OPN expression. We demonstrate the remarkable efficacy of OPN-siRNA to prevent EAU in mice.

2. Materials and methods

2.1. Experimental animals

6- to 8-week old female C57BL/6 (H-2^b; B6) mice were obtained from Japan SLC (Shizuoka, Japan). All studies were conducted in compliance with the Statement for the Use of Animals in Ophthalmic and Vision Research by the Association for Research in Vision and Ophthalmology (ARVO, Rockville, MD) and with the Hokkaido University Committee for Animal Use and Care.

2.2. Reagent

hIRBP (human interphotoreceptor retinoid-binding protein) peptide sequence 1–20 (GPTHLFQPSLVLDMAKVLLD) was purchased from Sigma-Genosys Japan (Ishikari City, Hokkaido, Japan). Purified *Bordetella pertussis* toxin (PTX) was purchased from Sigma–Aldrich (St. Louis, MO) and complete Freund's adjuvant (CFA) and *Mycobacterium tuberculosis* strain H37Ra were purchased from Difco (Detroit, MI).

2.3. Immunization

To analyze the cell proliferative response, $hIRBP_{1-20}$ (100 μg) was emulsified in CFA (1:1 v/v) and a total of 50 μl of the emulsion was injected subcutaneously (s.c.). To induce EAU, $hIRBP_{1-20}$ (200 μg) was emulsified in CFA (1:1 v/v) containing 2.5 mg/ml *M. tuberculosis* H37Ra. A total of 200 μl of the emulsion was injected s.c. concurrent with immunization, 0.1 μg of PTX in 100 μl phosphate-buffered saline (PBS) was injected intraperitoneally (i.p.) as an additional adjuvant (Kezuka et al., 1996).

2.4. Evaluation of EAU

Clinical assessment by funduscopic examination of the chorioretinal inflammation was carried out every 3 or 4 days from day 7 after immunization (Namba et al., 2000). The severity of EAU was graded 0–4 as described previously (Thurau et al., 1997). Briefly, the clinical scoring was based on vessel dilatation, the number of vessel white focal lesions, vessel white linear lesions and hemorrhages, and the extent of retinal detachment.

For the histological assessment of EAU, eyes were enucleated on day 21 after immunization. Removed eyes were fixed in 4% paraformaldehyde for an hour and transferred into 10% phosphate-buffered formaldehyde until processing. Fixed samples were embedded in paraffin and 5 μm sagittal sections were cut near the optic nerve head and stained with hematoxylin and eosin. The severity of EAU in each eye was scored on a scale of 0–4 as described previously (Caspi et al., 1988). In brief, no change was scored as 0. Focal non-granulomatous, monocytic infiltrations in the choroid, ciliary body, and retina were scored as 0.5. Retinal perivascular infiltration and monocytic infiltration in the vitreous were scored as 1. Granuloma formation in the uvea and retina, occluded retinal vasculitis, along with photoreceptor folds, serous retinal detachment, and loss of photoreceptors were scored as 2. In addition, the formation of granuloma at the level of the retinal pigmented epithelium and the development of subretinal neovascularization were scored as 3 and 4 according to the number and the size of the lesions.

2.5. Preparation of OPN- and control-siRNA

OPN- and control-siRNAs were purchased from B-Bridge (Sunnyvale, CA, USA). The sequences of sense and anti-sense strands of each siRNA were as follows: mouse OPN-RNAi-5/239: 5′-GCCAUGA CCACAUGGACGAdTdT-3′ (sense), 5′-UCGUCCAUGUGGUCAUGGCdT dT-3′ (anti-sense), control-siRNA pair, as designed to avoid specific sequences in mice; 5′-ACUCUAUCUGCACGCUGACUU-3′ (sense), 5′-GUCAGCGUGCAGAUAGAGUUU-3′ (anti-sense) (Saito et al., 2007). The siRNAs were deprotected, annealed and desalted.

2.6. In vivo treatment of mice with siRNA

Synthetic siRNAs were delivered *in vivo* using a modified hydrodynamic transfection method (Song et al., 2003), in which 50 μg of either OPN- or control-siRNA dissolved in 1 ml PBS was rapidly injected into the tail vein. Mice were treated with two injections of either OPN- or control-siRNA, 24 h before and simultaneously with the immunization (prevention regimen). Another group of mice was treated with two injections of either OPN- or control-siRNA on day 7 and day 8 after the immunization (reversal regimen).

2.7. Plasma OPN level

To quantify OPN concentration in plasma from EAU mice treated with either OPN-siRNA or control-siRNA, mice were deeply anesthetized with ether, and then blood was collected transcardially before immunization and on days 3, 7, 10, 14, 21, and 28 after immunization. All blood samples were collected in the presence of EDTA to avoid cleavage by thrombin *in vitro*, centrifuged to remove cells and debris, and stored at −80 °C. OPN concentration in plasma

samples (n = 24 mice) was quantified by an enzyme-linked immunosorbent assay (ELISA) kit for mouse OPN (Immuno-Biological Laboratories Co. Ltd., Takasaki, Japan) according to the manufacturer's protocol.

2.8. T cell proliferative responses

T cells obtained from B6 mice that had been primed with $hIRBP_{1-20}$ were cultured with Ag-presenting cells (APC) and $hIRBP_{1-20}$ as described elsewhere (Kitamura et al., 2007). In brief, T cell-enriched fraction was prepared as Nylon wool non-adherent cells by passing dispersed cells of draining lymph nodes from $hIRBP_{1-20}$-primed mice over nylon wool column. Then the T-enriched fraction (5×10^5/well) were co-cultured with mitomycin-C (MMC)-treated splenocytes as APC (5×10^5/well) and $hIRBP_{1-20}$ peptide at the indicated concentration in serum-free medium (RPMI 1640 medium), 10 mM Hepes, 0.1 mM non-essential amino acids, 1 mM sodium pyruvate, 50 μg/ml gentamicin sulfate, supplemented with 0.1% bovine serum albumin, and ITS + 1 liquid media supplement [2 μg/ml insulin from bovine pancreas, 1.1 μg/ml iron-free transferrin, 1 ng/ml sodium selenite, 100 μg/ml bovine serum albumin, and 1 μg/ml linoleic acid] (Sigma Chemical Co.). Cells in 96-well flat-bottomed plates were incubated for 64 h at 37 °C in 5% CO_2 in air, pulsed with 18.5 kBq of [^{3}H]-thymidine (Perkin Elmer Japan, Tokyo) per well during the last 16 h of incubation, and then were harvested. Incorporation of [^{3}H]-thymidine was quantified with a direct β-counter (Packard, Meriden, CT), and the data were presented as the mean counts per minute (CPM) minus the background (medium alone; ΔCPM) (Kitamura et al., 2007).

2.9. Quantification of cytokine

Cytokine concentrations in each culture supernatant were quantified with either BD™ Cytometric Bead Array kit (BD Bioscience, San Diego, CA, USA) (Cook et al., 2001) or FlowCytomix™ multiplex kit (Bender MedSystems GmBH, Vienna, Austria). In brief, as for CBA set-up, 50 μL samples or known concentrations of standard samples (0–5000 pg/ml) were added to capture beads conjugated with Ab for each cytokine followed by an addition of anti-cytokine Ab-phycoerythrin (PE) reagent (detection reagent). The mixture was then incubated for 2 h at room temperature in the dark, and washed to remove unbound detection reagent. As for FlowCytomix, 25 μL samples or known concentrations of standard samples (0–20 000 pg/ml) were added to capture beads conjugated with Ab for each cytokine followed by an addition of biotinylated anti-cytokine Abs and the mixture was incubated for 2 h at room temperature in the dark. After washing, the beads were incubated with streptavidin-PE for 2 h at room temperature in the dark, and washed to remove unbound detection reagent. Data acquisition was performed with FACS Calibur flow cytometer (BD Bioscience) and analyzed on a computer (CBA software 1.1; BD Bioscience or FlowCytomix Pro2.2 software). Amounts of IFN-γ, TNF-α and Interleukin (IL)-1α, -2, -4, -5, -6, -10, -17, and granulocyte macrophage colony-stimulating factor (GM-CSF) were quantified.

2.10. Statistical analysis

Data are presented as mean ± SD in clinical and histopathological scoring and as mean ± SEM in analyses of cell proliferation and cytokine production. Statistical analysis of EAU scoring was performed using the nonparametric Mann–Whitney U-test. Analyses of cell proliferation and cytokine production were performed using two-tailed Student's t-test. P values < 0.05 were considered statistically significant.

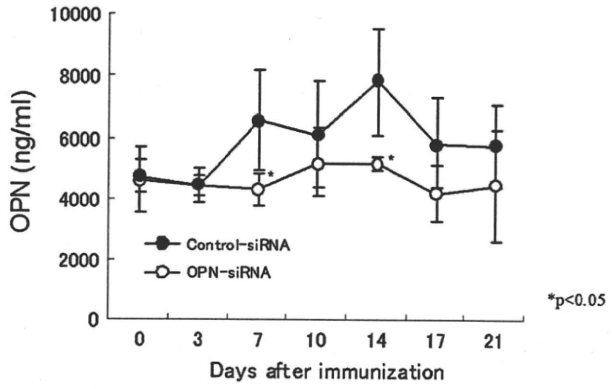

Fig. 1. Persistence of inhibition of plasma OPN level following *in vivo* siRNA treatment during EAU. EAU was induced in B6 mice. These mice were treated with OPN-siRNA (○) or control-siRNA (●) with hydrodynamic methods 24 h before and simultaneously with immunization. Blood was collected transcardially before immunization and on days 3, 7, 10, 14, 17 and 21 after immunization from each group of mice. All blood samples were collected under EDTA, centrifuged to remove cells and debris, and stored at −80 °C until used. Plasma levels of OPN were measured by sandwich ELISA. The results are presented as mean ± standard deviation. Statistical significance was determined using two-tailed Student's t-test (**, $P < 0.01$, *, $P < 0.05$). Data are representative of two separate experiments with the same result.

3. Results

3.1. OPN-siRNA treatment inhibited the increase of OPN plasma level during EAU

We demonstrated that the plasma concentration of OPN elevated from the basal level (4–5 μg/ml) over time after $IRBP_{1-20}$, peaked around 14 d, and then gradually waned (Kitamura et al., 2007), suggesting that plasma OPN concentration correlates well with disease development. First, we quantified the plasma OPN level to examine whether administration of OPN-siRNA could actually reduce the OPN level *in vivo*. To this end, we introduced siRNA twice at 24 h before and at the same time of $IRBP_{1-20}$ immunization. In the control-siRNA-treated group, OPN concentration in plasma again peaked around 2 wk, thus reproducing our previous results. On the other hand, in the OPN-siRNA-treated group, the OPN concentration in plasma was not elevated from the basal level during EAU. In comparison with that of the control group, plasma concentration of OPN upsurge was significantly

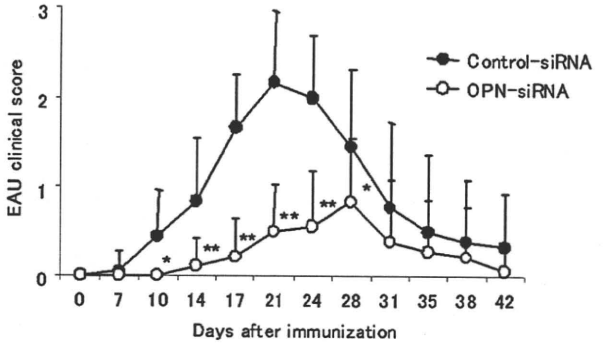

Fig. 2. Clinical score of EAU in mice treated with OPN-siRNA, 24 h before and simultaneously with the immunization. EAU was induced in B6 mice. These mice were treated with OPN-siRNA (○) or control-siRNA (●). Funduscopic examination was carried out every 3 or 4 days from day 7 after immunization. The results are presented as mean clinical score for all eyes of each group of mice (9 mice per group) ± standard deviation. Significance was determined using Mann–Whitney U-test (**, $P < 0.01$, *, $P < 0.05$).